Final Report (9/15/90 - 10/15/93)

TRANSIENT INTERNAL PROBE
AFOSR-90-0345

Submitted to

AIR FORCE OFFICE OF SCIENTIFIC RESEARCH
PLASMA PHYSICS BRANCH
BOLLING AIR FORCE BASE
WASHINGTON, D.C. 20332

December 15, 1993

UNIVERSITY OF WASHINGTON
Aerospace and Energetics Research Laboratory, FL-10
Seattle, Washington 98195

Professor Thomas R. Jarboe
Principal Investigator

DISCLAIMER NOTICE

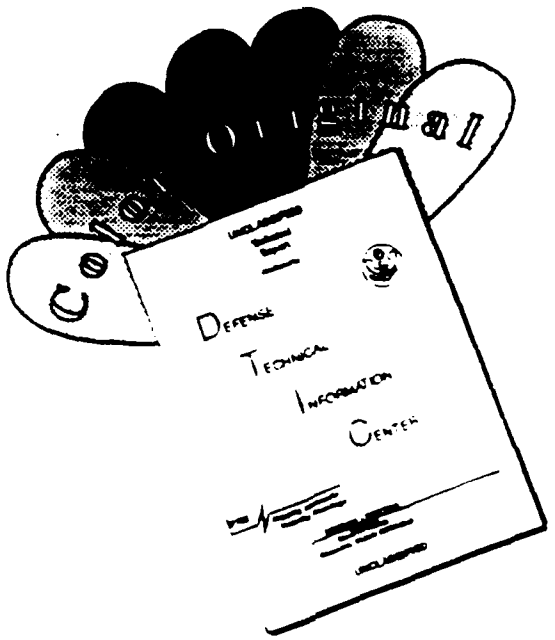

THIS DOCUMENT IS BEST QUALITY AVAILABLE. THE COPY FURNISHED TO DTIC CONTAINED A SIGNIFICANT NUMBER OF COLOR PAGES WHICH DO NOT REPRODUCE LEGIBLY ON BLACK AND WHITE MICROFICHE.

unclassified
SECURITY CLASSIFICATION OF THIS PAGE

REPORT DOCUMENTATION PAGE

1a. REPORT SECURITY CLASSIFICATION: unclassified	1b. RESTRICTIVE MARKINGS:
2a. SECURITY CLASSIFICATION AUTHORITY:	3. DISTRIBUTION/AVAILABILITY OF REPORT: ⊗ unlimited
2b. DECLASSIFICATION/DOWNGRADING SCHEDULE:	
4. PERFORMING ORGANIZATION REPORT NUMBER(S):	5. MONITORING ORGANIZATION REPORT NUMBER(S):
6a. NAME OF PERFORMING ORGANIZATION: Aerospace & Energetics Research Program; 6b. OFFICE SYMBOL (If applicable): FL-10	7a. NAME OF MONITORING ORGANIZATION: Air Force Office of Scientific Research
6c. ADDRESS (City, State and ZIP Code): University of Washington, Seattle, Washington 98195	7b. ADDRESS (City, State and ZIP Code): Bolling Air Force Base, D.C. 20332-6448
8a. NAME OF FUNDING/SPONSORING ORGANIZATION: AFOSR; 8b. OFFICE SYMBOL (If applicable): /NE	9. PROCUREMENT INSTRUMENT IDENTIFICATION NUMBER: AFOSR-90-0345
8c. ADDRESS (City, State and ZIP Code): Building 410, Bolling Air Force Base, D.C. 20332-6448	10. SOURCE OF FUNDING NOS. — PROGRAM ELEMENT NO.: 61102F; PROJECT NO.: 2301; TASK NO.: A8; WORK UNIT NO.:
11. TITLE (Include Security Classification): (unclassified) TRANSIENT INTERNAL PROBE DIAGNOSTIC	
12. PERSONAL AUTHOR(S): JARBOE, Thomas R.; MATTICK, Arthur T.	
13a. TYPE OF REPORT: final technical report; 13b. TIME COVERED: FROM 90/9/15 TO 93/10/15; 14. DATE OF REPORT (Yr., Mo., Day): 1993 December 15; 15. PAGE COUNT: 56	
16. SUPPLEMENTARY NOTATION: n/a	

17. COSATI CODES		
FIELD	GROUP	SUB. GR.

18. SUBJECT TERMS (Continue on reverse if necessary and identify by block number): transient internal probe; magnetic fusion diagnostic Verdet material; Faraday rotator material; polarization measurements; 2-stage light gas gun; diamond ablation

19. ABSTRACT (Continue on reverse if necessary and identify by block number)

The Transient Internal Probe (TIP) diagnostic is a novel method for probing the interior of hot magnetic fusion plasmas that are inaccessible with ordinary stationary probes. A small probe of magneto-optic (Verdet) material is fired through a plasma at speeds of several km/sec, illuminated by a laser beam. The beam's polarization is rotated in the probe by the local magnetic field and retroreflection back to a polarimetry detector allows determination of the B-field profile across the diameter of a plasma at a spatial resolution of better than 1-cm and an absolute B-field resolution of a few tens of Gauss.

The principal components of a TIP diagnostic system were developed and tested. A two-stage light gas gun was constructed that accelerates 30-caliber projectiles to 3 km/sec, and methods were examined for stripping a lexan sabot from a probe prior to entry into a plasma. Probes of CdMnTe and FR-5 Verdet glass were fabricated, and a polarimetry system was constructed for resolving polarization to within 0.25°. The diagnostic was validated by measuring a static B-field with a moving (dropped) TIP probe, and finding agreement with Hall-probe measurements to within experimental accuracy (40 gauss).

20. DISTRIBUTION/AVAILABILITY OF ABSTRACT: UNCLASSIFIED/UNLIMITED ☒ SAME AS RPT. ☐ OTIC USERS ☐	21. ABSTRACT SECURITY CLASSIFICATION: unclassified
22a. NAME OF RESPONSIBLE INDIVIDUAL: ~~JARBOE, Thomas R.~~ Barker	22b. TELEPHONE NUMBER (Include Area Code): ~~206-685-3427~~ 202-767-5011; 22c. OFFICE SYMBOL: ~~FL-10~~ NE

DD FORM 1473, 83 APR — EDITION OF 1 JAN 73 IS OBSOLETE.

unclassified
SECURITY CLASSIFICATION OF THIS PAGE

TRANSIENT INTERNAL PROBE

SUMMARY

This is a final report on the work carried out on the Transient Internal Probe (TIP) diagnostic experiment under the Air Force Office of Scientific Research Grant # AFOSR-90-0345. The period of this work was 9/15/90-10/15/93.

The TIP diagnostic is a novel method for probing the interior of hot magnetic fusion plasmas that are inaccessible with ordinary stationary probes. In the TIP scheme, a small probe constructed of a magneto-optic material is fired through a hot plasma at high velocity. During its transit the probe is illuminated with polarized laser radiation, which passes through the probe and is retroreflected back to the source by means of a reflector mounted on the probe's back face. In the double pass through the probe, the light's polarization is rotated in proportion to the local magnetic field, and resolution of the polarization angle of the return light by a detection system remote from the plasma allows accurate determination of the magnetic field. In hotter plasmas the probe can be encased in a refractory material, such as diamond, to minimize ablation.

Under this grant, an experimental program was carried out to develop and test the major components needed to accelerate a small magneto-optic probe crystal into a plasma, to direct a laser signal to the probe and detect and analyze the reflected return signal, and to process the data for determining local magnetic fields. The successful development of these components has validated the utility of the TIP concept, and the equipment which was developed can readily be incorporated into a diagnostic system for measuring magnetic fields in research plasmas.

A two-stage light gas gun for accelerating probes into a plasma chamber was designed, constructed and tested. Projectile velocities of 3 km/sec have been obtained using 30-caliber lexan sabots and 4-mm-square glass probes using helium as a driver gas. This speed is suitable to insure survival of the probe as it traverses the HIT plasma at the University of Washington. Scaling these results to the maximum breech pressure, it is expected that speeds of 4.5 km/sec should be obtainable, for use with hotter plasmas. Designs for sabot-stripping and for interfacing the gun to a plasma device were developed during the grant period, although time constraints prevented testing of these designs.

An optical system was constructed for illuminating the TIP probes with laser radiation, and a polarimeter was constructed and optimized for analyzing return light from probes. The sensitivity of the polarimeter is 0.25° in polarization angle, competitive with polarimetry systems used on other plasma experiments. This provides a capability for resolution of local magnetic fields of approximately 40 gauss, when probes of FR-5 Verdet material are illuminated with 628 nm radiation from a He-Ne laser.

Faraday rotator probes have been constructed out of both Terbium-doped Borosilicate (FR-5 glass) and Manganese-doped Cadmium Telluride (CdMnTe). Although the CdMnTe probes have a higher Verdet coefficient than the glass, the high index of refraction and birefringence of the CdMnTe material was found to degrade the sensitivity. Transient measurements of a magnetic field using FR-5 probes have been carried out using the polarimeter to analyze the Faraday-rotated light. These TIP probe measurements were found to be reproducible and agree well with measurements made using a stationary Hall probe.

TABLE OF CONTENTS

TRANSIENT INTERNAL PROBE

T.R. Jarboe and A.T. Mattick
University of Washington

1. INTRODUCTION

This report presents the results of the work performed under Air Force Office of Scientific Research Grant # AFOSR-90-0345, to develop a new diagnostic technique, the Transient Internal Probe (TIP), for measuring local magnetic fields in research plasmas. This work was carried out at the University of Washington during the period 9/15/90 to 10/15/93.

This introduction presents the background motivation for developing this new diagnostic, and summarizes the research objectives and accomplishments of the program. The following chapters describe in detail the results of the development and testing of the principal components of the TIP apparatus.

1.1 Background

A critical problem in the study of plasmas is the measurement of local magnetic fields. Although external field measurements can provide global information on current distributions, for example, many of the processes that are pivotal for characterizing plasmas take place at a scale that is orders of magnitude smaller than the plasma dimensions, and are inaccessible with the use of external probes. Local processes involving fluid motion, plasma waves, plasma heating and transport must often be inferred from global information and computer simulation. Knowledge of local fields can provide direct insight into these processes, and internal probes have been used wherever possible to obtain this information. To date, the utility of internal probes has been constrained by materials limitations. The large heat transport to probes in hot plasmas limits probe lifetime, and evaporation of probe material can easily "poison" a plasma by introduction of high-Z material. For this reason, probes are often confined to the cooler, edge regions of a plasma. Transient probing, where probes are mechanically inserted and withdrawn over periods of 50-100 msec, has been used,[1] but, again, this is usually confined to the plasma edge.

The Transient Internal Probe is a new diagnostic method developed at the University of Washington which minimizes or avoids these problems in the measurement of magnetic fields in hot plasmas.[2-6] The TIP concept, illustrated in Fig. 1.1, makes use of a free-flying probe made of magneto-optic material that traverses a plasma in sub-millisecond time scales, short enough that probe evaporation is minimal or nonexistent. In very hot and dense plasmas the probe can be encased in a diamond enclosure to insure survival. The magneto-optic probe material has the characteristic of rotating the polarization of light in proportion to the local magnetic field. The strength of the field at the instantaneous position of the probe is measured by illuminating the probe with polarized laser radiation, and measuring the angle of polarization rotation in light that returns to a detection system by a retroreflection off of the probe's back face. Communication of field information via visible, narrow-band radiation has advantages of high sensitivity, high bandwidth, and minimal interference by the plasma itself. Detectors can be placed far from the plasma, and can be isolated from the effects of plasma-generating equipment. Relatively common magneto-optic (Verdet) materials exist that allow good field resolution (<40 gauss) using sub-centimeter probe dimensions. The high sensitivity to local fields, and the ability to map out the magnetic field over a plasma diameter in sub-millisecond time scales, represents a breakthrough in plasma diagnostics that will enable direct characterization of plasma processes that have heretofore been difficult or impossible to access.

The understanding of the equilibrium, stability, and transport of a magnetized plasma will be greatly improved by accurate measurement of local fields and their fluctuations. Use of TIP will increase the bandwidth for B-field fluctuations by a factor of 1000 above normal internal probes. However, the primary advantage of TIP is the ability to probe higher temperature and long-lived plasmas: the exposure time of a TIP probe can be 100 times shorter than that of present reciprocating probes, and the exposed area can be 100 times smaller than that of normal probes. The small size of TIP probes makes it feasible to encase them in diamond to enhance the lifetime in hot plasmas. For example, present probing in fusion research is limited to edge plasmas of 50 eV. This new technology would allow measurements in 1.9 keV plasmas.[2] Thus, the internal magnetic fields and their fluctuations could be measured throughout the entire volume of DIII-D (a leading fusion tokamak), not just in the edge. This data is desperately needed by fusion research for understanding stability and transport.

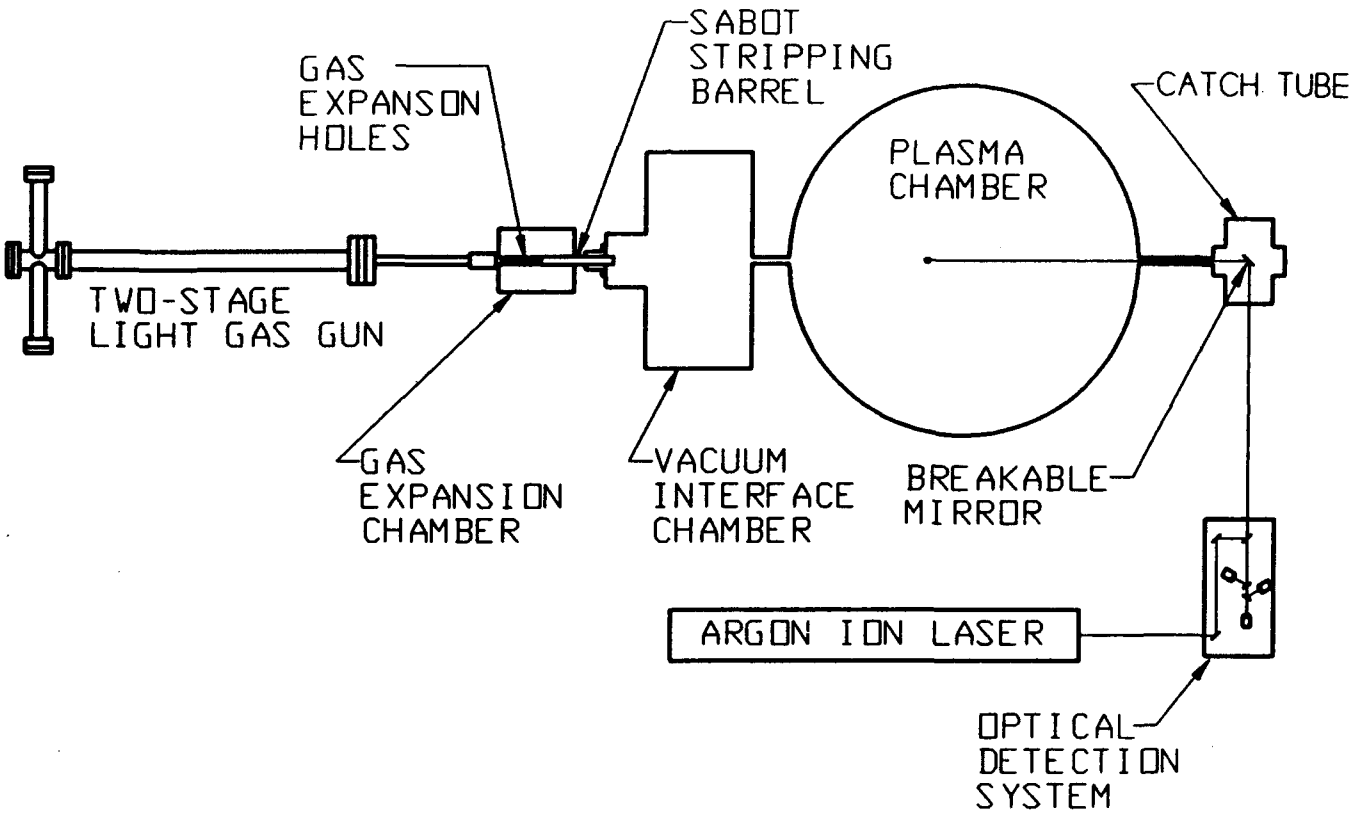

Fig. 1.1 Schematic of TIP concept.

1.2 Research Objectives

The objectives of this program were to develop and test the primary components of a TIP diagnostic system, and to demonstrate the capability of this system for measuring magnetic fields. The components of the system include a 2-stage light gas gun for accelerating Verdet probes (held by sabots) to speeds of several km/sec, a sabot-stripping scheme to separate the probe from its sabot prior to injection into a plasma chamber, the magneto-optic probes, and a laser illumination system and polarimeter for analyzing the polarization of retroreflected light. Additional equipment was also developed for measuring probe speed, imaging probes, and analyzing data.

1.3 Summary of Research Results

The primary components of a TIP diagnostic system were successfully constructed and tested, although sabot-stripping schemes could not be completed by the end of the program. Tests were carried out to measure a magnetic field using a moving TIP probe, which yielded field strengths in agreement with a Hall probe, thus validating the TIP concept. With further development the TIP apparatus can be interfaced with plasma experiments to enable high-resolution measurements of local magnetic fields in plasmas. The following subsections summarize the work on each of the major TIP components.

1.3.1 Two-stage light gas gun

A 2-stage light gas gun has been designed, constructed and tested. Using Nitrogen as the propellant gas, a 1.5 km/sec projectile velocity has been measured using a fast image-converting camera. By switching to a lighter propellant gas, helium, projectile velocities of 3.0 km/sec have been measured using both a ballistic pendulum and a laser-interruption scheme as well as by imaging, with all speed diagnostics in agreement. The breech pressure during these shots was measured to be 42000 psi, about half the maximum pressure of 80000 psi at which the gun was designed to operate safely. At the maximum pressure rating a velocity of 4.5 km/sec should be attainable.

1.3.2 Sabot stripping

Two designs have been examined for separation of the sabot from a TIP probe to prevent sabot material from entering a plasma experiment. The first and simplest to

implement is an axial stripping scheme, whereby a constriction downstream of the gun muzzle stops the sabot but allows the probe to pass freely. The second scheme, radial stripping, uses a segmented sabot and a rifled barrel. Centrifugal force causes the sabot segments move radially away from the probe when the projectile emerges from the barrel. Radial stripping has been demonstrated to work reliably in other ballistics research, but is more complicated in that it requires a rifled and vented gun barrel, a more complex sabot, and a method of preventing the sabot obturator from entering the plasma. The delay in getting the gas gun to work reliably with helium prevented testing of these stripping schemes.

1.3.3 Faraday probes

Faraday probes were constructed using Terbium-doped Borosilicate glass (FR-5) and Manganese-doped Cadmium Telluride (CdMnTe). Both materials can be obtained commercially, fabricated to TIP probe specifications. The FR-5 probes were successfully used to make transient magnetic field measurements, but the CdMnTe probes were found to have too high a reflection coefficient and birefringence to be useful for TIP applications, despite the use of antireflection coatings. Corner-cube reflectors were originally used to retroreflect laser light back to the detection system. However, retroreflecting sheet material was found to perform satisfactorily, and results in a lighter, more compact probe which better withstands the forces of acceleration.

1.3.4 Laser illumination and detection system

An optical system for illumination and tracking of a TIP probe with a He-Ne laser has been set up, and a polarimetry system has been constructed which utilizes three detectors to achieve a resolution in polarization angle of 0.25°. The 3-detector design insures that the sensitivity is maintained for all polarization angles. An 8-bit, 10-MHz data acquisition system has been set up which is capable of recording the polarization signals at the speed and sensitivity needed for plasma field measurements, and software has been written and tested for extracting magnetic field data from the signals.

1.3.5 Diamond ablation experiment

Diamond ablation studies were performed to determine the effect of hot plasmas on the proposed diamond cladding for TIP projectiles. It is known that materials injected into a fusion experiment will suffer ablation as they interact with the hot plasma. This effect is used in fueling plasmas, by injecting pellets of deuterium or

tritium. While ablation rates for these materials are fairly well known, there is not an experimental data base for ablation rates of diamond. To study these rates, small diamond pellets were injected into the Madison Spherical Torus (MST) and the ablative effects measured. These measurements indicate an ablation rate for diamond that is significantly less than that of carbon.

1.4 Personnel

Professor Tom Jarboe, now of the Department of Aeronautics and Astronautics was the Principal Investigator for the program, with overall responsibility for technical management. Dr. Greg Spanjers, a postdoctoral associate in the Department of Nuclear Engineering was the lead investigator during the first two years of the program. Professor Tom Mattick of the Aeronautics and Astronautics Department assumed supervision of experimental program in January, 1993. Professor Glen Wurden was primarily responsible for the diamond ablation studies. The light gas gun was designed and constructed by Mike Bohnet as a Master's thesis under guidance of Prof. Walter Christiansen of the A&A Department, and the laser illumination and detection system was developed by Jim Galambos, also for a Master's thesis.

1.5 Publications

The publications on the TIP diagnostic which were made in the course of this grant are listed below.

G.G. Spanjers, et.al., "Development of a transient internal probe diagnostic," Rev. Sci. Instrum. 63, 5148 (1992). [Attached as Appendix A]

G.G. Spanjers, et.al., "Development of a transient internal probe diagnostic," presented at 9th Topical Conference on High-Temperature Plasma Diagnostics, Santa Fe, N.M., March 15-19, 1992.

G.G. Spanjers, J.P. Galambos, M.A. Bohnet, and T.R. Jarboe, "Magnetic field measurements using the transient internal probe," presented at the APS Plasma Physics Conference, Seattle, WA, Nov. 16-20, 1992.

J.P. Galambos, "Remote magnetic field measurements using an optically coupled probe," M.S. Thesis, Univ. of Wash., Dept. of Nuclear Engineering, January, 1993.

M.A. Bohnet, "Development of a two-stage light gas gun," M.S. Thesis, Univ. of Wash., Dept. of Aeronautics and Astronautics, June, 1993.

2. TWO-STAGE LIGHT GAS GUN

The utility of the TIP concept derives from the ability to transmit a probe through a hot plasma in times short enough that the probe will not degrade due to heating. A speed of 2 km/sec was the original target for this program, primarily as a demonstration of the concept. This speed is sufficient for utilizing the TIP probe for magnetic field measurements on the Helicity Injected Tokomak (HIT) plasma device at the University of Washington. For maximum utility, however, it would be advantageous to achieve speeds in excess of 2 km/sec, and speeds up to 5 km/sec are achievable with the use of 2-stage light gas guns.[7] The design, construction, and testing of such a gun was a key element of the program, and it has been possible to achieve speeds of nearly 3 km/sec, with an ultimate speed capability for our device projected to be as high as 4.5 km/sec. Details of the gun's design can be found in Ref. 5. The following sections summarize the development and testing.

2.1 Basic Description of Gun Operation

The gun has evolved through a series of design changes during the program. A schematic of the final design is illustrated in Fig. 2.1. The gun is energized by a nitrogen "driver gas", pressurized to nominally 1600 psi in driver tubes mounted perpendicularly to a pump tube. The symmetrical driver tubes are each 56-cm long, by 7.6-cm ID, and are constructed of carbon steel to facilitate welding. When the gun is fired, the driver gas pushes a piston down a 2.44-m long by 4.0-cm ID pump tube constructed of 4340 alloy steel, which is filled with a "pump gas" to nominally 40 psi. A 30-caliber gun barrel is mounted to the end of the pump tube, separated from the pump gas by a scored diaphragm. As the piston traverses the pump tube, it pressurizes the pump gas to a level sufficient to burst the diaphragm (nominally 50,000 psi), releasing the gas against the projectile (30-caliber sabot, holding a sub-caliber TIP probe) to accelerate it down the 5-foot-long gun barrel. The use of a 2-stage gun provides a much higher velocity potential than simply using a statically pressurized gas to accelerate a projectile.

This gun incorporates several novel features which enhance reliability, and minimize wear. To avoid the use of fast-acting valves to activate the driver tubes, the piston is placed at the driver/pump interface before firing. The symmetrical, radial driver pressure on the piston results in a zero axial force, and seals prevent leakage of driver gas into the pump tube or to the region behind the piston. To fire the gun, the space

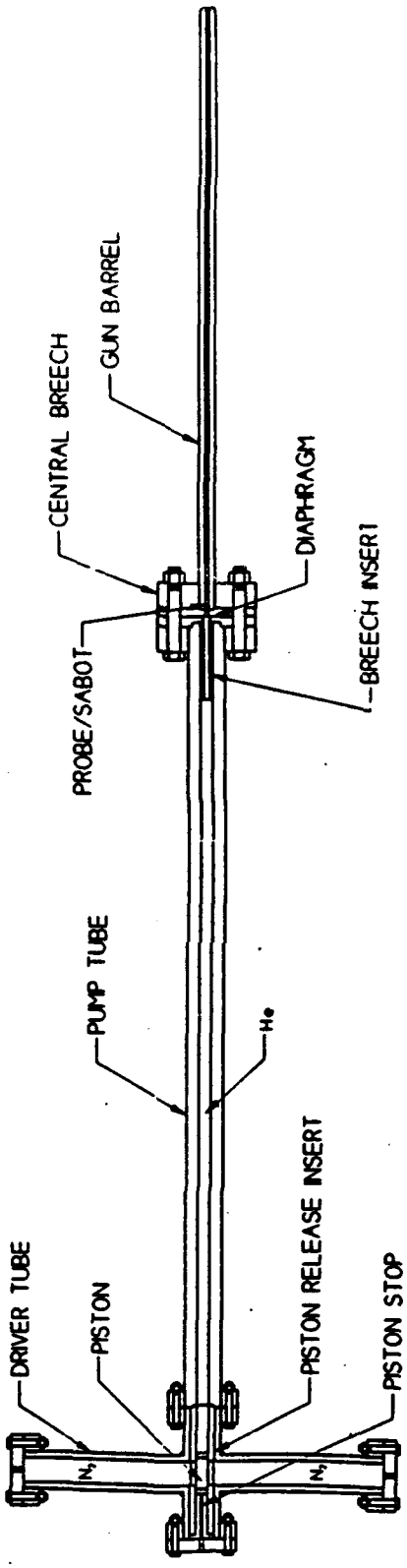

Fig. 2.1 Schematic of two-stage light gas gun.

behind the piston is pressurized to about 1600 psi, moving the piston forward. When the back of the piston has cleared the driver-to-pump interface holes, the driver gas begins acting on the back face of the piston to accelerate it down the pump tube.

A second design feature which minimizes wear and enhances the gun's life is the use of the pump gas pressure to decelerate the piston to rest, rather than using mechanical stops. This idea can be conveyed by considering a plugged pump tube, such that the pump gas is always confined. When the pump gas pressure exceeds the driver gas pressure, the piston begins to decelerate, although the piston inertia continues to pressurize the helium. The rate of deceleration increases as the helium pressure continues to rise, and at some point the piston stops and begins to accelerate backwards. Without frictional losses, the piston would oscillate indefinitely in the tube, but in practice the piston comes to rest after a few oscillations. The gun is designed to reverse piston motion before end-wall contact in the normal gun operating mode (diaphragm bursts), by suitably choosing the driver and pump-tube volumes and fill pressures, and diaphragm. To minimize damage to the pump tube in case of a leak or premature diaphragm burst, the piston cross-section is "coke-bottled", allowing expansion space during deceleration and, the piston is constructed of a metal (aluminum bronze) dissimilar from the pump tube (alloy steel) to avoid cold welds and galling.

The gun was designed from the beginning to be modular, allowing easy assembly and disassembly of its components. The major sections - driver tube, pump tube, and barrel - are joined together with bolted flange connections. To minimize cost, the flanges for the bolted connections are not machined from the same stock as the tube; rather they are designed to be screwed on to the ends of the tubes. Both the tubes and the flanges are over-designed with high safety factors, not only for stress reduction, but also for minimum elastic displacement under loads, which insures proper performance of seals. The bolted connections are also designed such that a significant compressive load still exists on the joint when maximum pressure occurs in the tube. The driver tube has been hydrostatically tested to 5000 psi, and the pump tube and barrel to 80000 psi.

The 900-lb gun has been installed on a hydraulically-powered positioning mount to facilitate alignment with test facilities downstream. Pressurization and firing of the gun is carried out remotely for safety reasons, using electrically-operated valves. A schematic of the gas-handling system is shown in Fig. 2.2, and a photograph of the gun is shown in Fig. 2.3. Setup time between firings is approximately 1 hour.

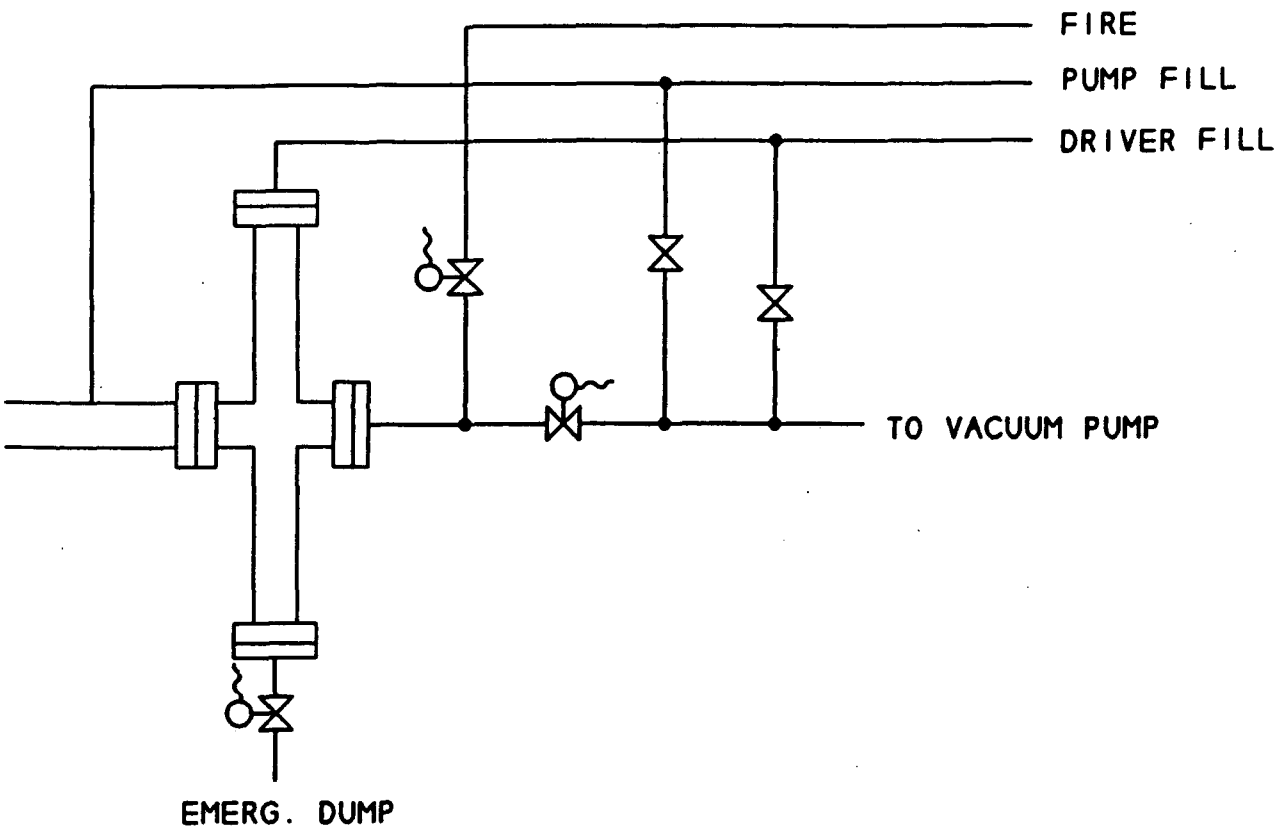

Fig. 2.2 Schematic of TIP gas-handling system.

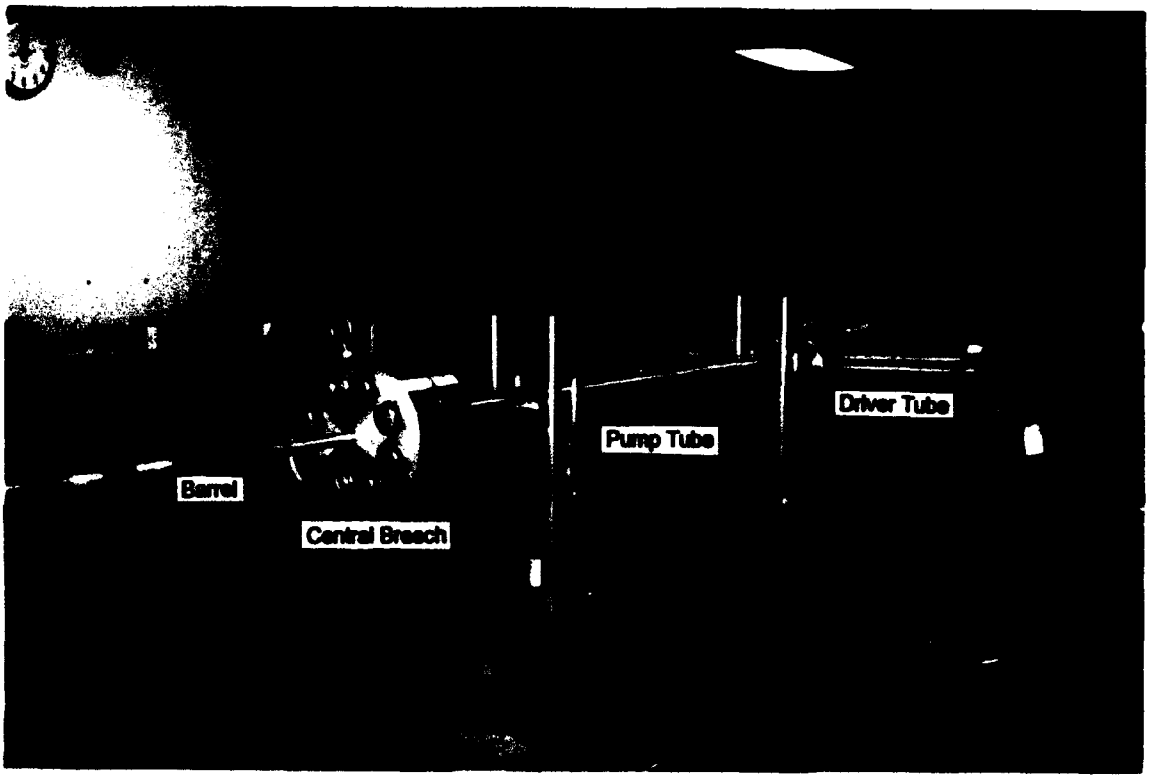

Fig. 2.3 Photograph of two-stage light gas gun.

In the initial development of the gun, nitrogen was used as a pump gas for checking out its operation. Once the gun performed satisfactorily with nitrogen, helium was used to achieve higher projectile velocities. The following sections describe the results for the use of these two gases, and the modifications necessary when using helium.

2.2 Operation of the Light Gas Gun with Nitrogen Propellant

Following construction and hydrostatic testing of gun components, the operation of the driver and pump tubes was tested using nitrogen pump gas with the pump-tube end blocked off with an end piece containing a piezoelectric pressure transducer. By varying the pump tube fill pressure, we found that a fill pressure ratio (driver pressure/pump pressure) of 21 would fully decelerate the first stage piston just as it reached the insert at the end of the pump tube. The upper trace of Fig. 2.4 shows the breech pressure for a 2000 psi driver fill pressure. The maximum breech pressure is approximately 50,000 psi with a single-stroke piston travel time of 22 msec. The following smaller peaks are produced as the piston oscillates back and forth in the pump tube, compressing and expanding the propellant gas.

After an accurate measurement of the breech pressure, the next step was to develop a suitable diaphragm between the pump tube and the barrel that would remain closed until the maximum breech pressure was created and then burst, allowing the propellant gas to accelerate the projectile. Scoring of the diaphragm to achieve desired burst pressure was determined by trial and error, starting with tables from Ref. 8. The optimized diaphragm developed for the TIP gun is 0.080"-thick 304 annealed stainless steel, scored to a 0.022" depth. The lower trace of Fig. 2.4 shows the breech pressure history with the diaphragm in place. The pressure build-up is quite similar for the upper and lower traces of Fig 2.4, although the 42,000 psi peak pressure with the diaphragm in place is somewhat lower than the 50,000 psi peak with the pump tube blocked. The measurements were repeated numerous times and found to be reproducible.

For the final phase of performance testing with nitrogen, we reinstalled the gun barrel, fired 0.7-gram lexan projectiles and measured the projectile velocity. The velocity was measured using two techniques. The first was to use a high-speed framing camera to photograph the projectile at set time intervals of 10 μsec. The velocity is determined from the projectile displacement between frames. The second technique used wires mounted on baffles, which had been placed downstream of the

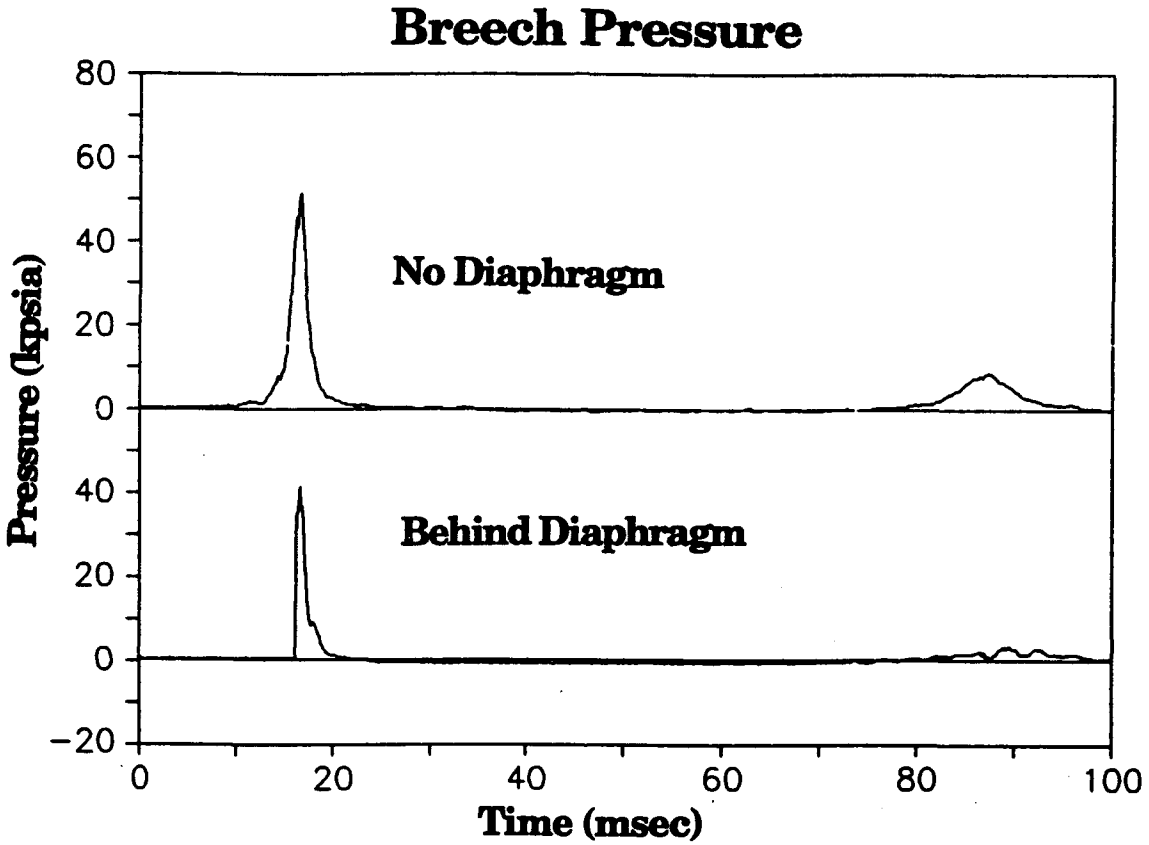

Fig. 2.4 Pressure transducer traces from the 2-stage light gas gun. The upper trace shows the breech pressure history with the pump-tube blocked off using a pressure ratio of 21 and a 2000 psi fill pressure for driver gas. The lower trace shows pressure history with diaphragm in place.

barrel to minimize muzzle blast. Interruption of current in the wires indicated projectile position, and was also used for triggering the camera.

Fig. 2.5 shows three photographs of the projectile taken by the camera at 10 μ sec intervals. The velocity calculated from the photographs is 1.5 km/sec. The photographs also show no sign of projectile wobble or instability at 1 meter from the muzzle. The velocity determined from wire breakage was 1.8 km/sec, and it was determined that the shock-wave ahead of the projectile, rather than the projectile itself, was prematurely breaking the wires. Evolution of the shock ahead of the projectile leads to uncertainty in the true projectile speed.

2.3 Operation of the Light Gas Gun with Helium Propellant

Once satisfactory operation of the gun was obtained with nitrogen, helium was used as a propellant, to increase the projectile speed. Initially all the geometrical parameters, such as the breech insert dimensions, were to be the same as in the nitrogen tests. The operation of the gun using helium proved to be more difficult than with nitrogen. The small atomic size and high temperatures are thought to be the cause of the helium leaking past the piston seals much more readily than in the nitrogen case. On the first test shot using helium, the steel piston collided with the insert, causing expansion of the piston inside of the pump tube. This expansion caused the piston to permanently lodge itself in the pump tube. The collision occurred because the hot pressurized helium gas that was supposed to slow the piston down, leaked past the piston seals. As a result, the piston was redesigned.

The revised piston design utilized aluminum-bronze instead of steel, with an extra Poly-Pak seal on the front end to help prevent leakage during the compression stroke. The change of materials from steel to bronze was to facilitate removal of the piston in case of future collisions, since cold welds would not happen between dissimilar metals. The ease of piston removal was also furthered by axially tapering the new design to minimize the contact area with the pump tube.

A new pump tube was obtained, having a smaller fill hole to reduce seal wear, and was compression tested with helium. Calculations were carried out which predicted an optimum pressure ratio of 37, to reach a peak breech pressure of 50,000 psi, with the piston coming to rest just as it reaches the breech insert. The higher pressure ratio, compared to the nitrogen case, results from helium's lower specific heat and higher gamma. A series of tests were conducted, gradually raising the pressure

Fig. 2.5 Photographs of TIP projectile (lexan sabot, 7.6-mm dia, 12-mm long, 0.7 gm) fired from TIP gun with nitrogen pump gas. The three exposures are taken 10 μsec apart.

ratio up to a value of 37. Unfortunately, the maximum breech pressure was found to be significantly less than predicted in these tests, and the cause was found to be helium leakage.

To rectify this, the pump-tube insert was shortened and the piston seal was changed from a Poly-Pak seal to a Bridgeman seal. The latter greatly reduced the leakage, and this seal also serves an excellent cushion for impact of the piston with the insert. The Bridgeman seal is replaced every shot and is designed to be easy to fabricate and inexpensive. A hole drilled into the end of the piston is used to hold the Bridgeman seal and can be threaded if needed to facilitate removal of a stuck piston. The lower yield strength of Brass makes this unlikely. Fig. 2.6 shows a photograph of the new piston, the Bridgeman seals, and lexan projectiles. Using the piston with the Bridgeman seal, the driver/pump-tube combination reproducibly produced a maximum breech pressure of 42,000 psi using a driver fill pressure of 1600 psi and a pressure ratio of 38. The maximum breech pressure was kept to 42,000 psi instead of 50,000 psi because of occasional leakage past the static O-ring seals in the breech of the gun, due to the high helium temperature. Finding a suitable diaphragm that would open reproducibly at 42,000 psi proceeded as before. The required scoring depth was found to be 0.026".

Measuring the velocity of projectiles with helium pump gas proved to be more difficult than with nitrogen, primarily because the higher temperature of the helium resulted in significant conduction of current after the wires downstream of the muzzle were broken. This led to unreliable triggering of the imaging camera. A ballistic pendulum was therefore built for velocity measurement. This was simply a catcher tube of known mass, suspended by string from a fixed mount. The projectile speed can be determined from the amplitude of oscillation of the pendulum following a shot. Using the pendulum, the projectile speed was measured to be 3 km/sec with a spread of 200 m/sec, for the nominal fill pressures of the gun.

Subsequently a new method for velocity measurement was implemented using the interruption of a He-Ne laser beam by the projectile at two stations downstream of the muzzle. Interruption of the beam nearest the muzzle was also used to trigger the high-speed camera for additional data on projectile velocity. Figure 2.7 shows successive images taken with the camera, and Fig. 2.8 show traces of the He-Ne laser signal during a shot. All three velocity determinations were found to agree to within about 5%.

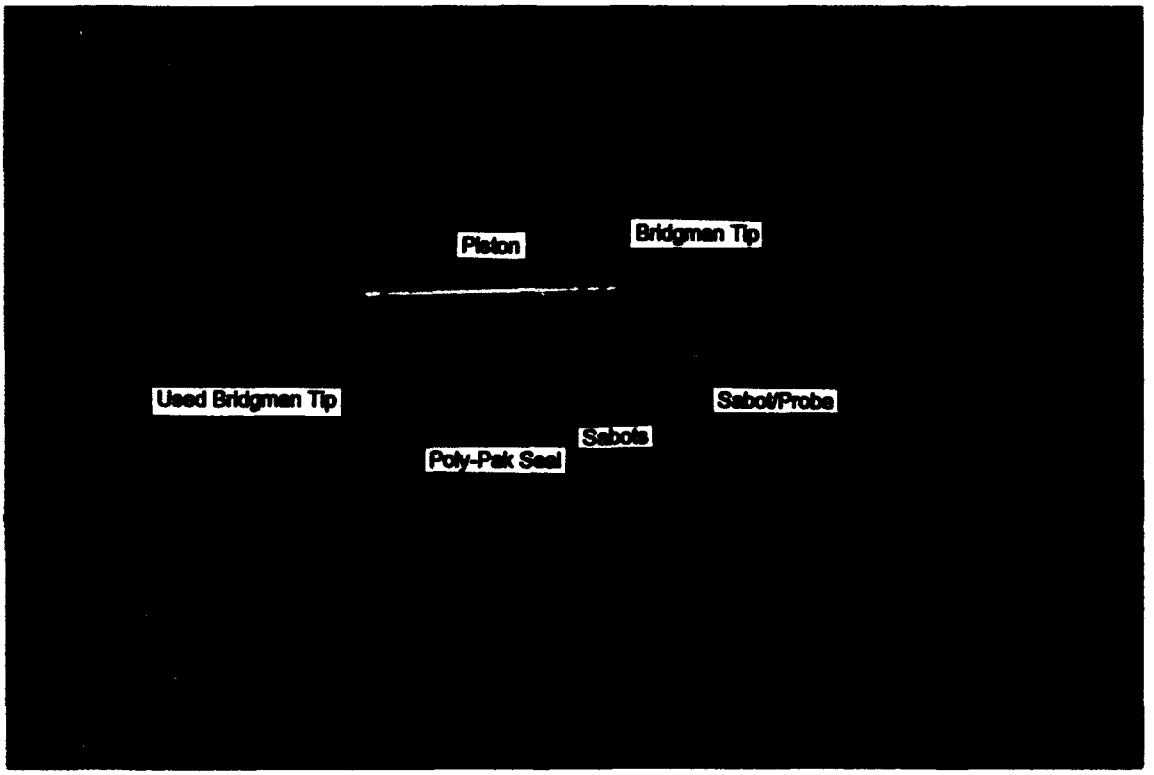

Fig. 2.6 Photograph of revised piston design for helium pump gas, including Bridgeman seals and lexan projectiles.

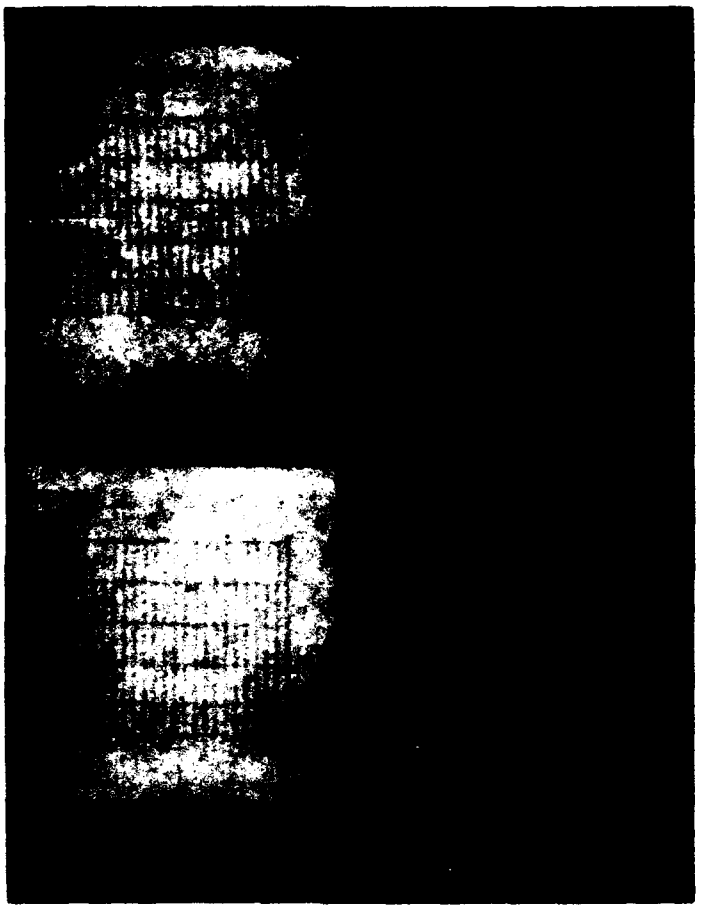

Fig. 2.7 Photographs of lexan sabot in flight using helium pump gas. Frames are taken 10 μsec apart, and projectile speed is 2.75 km/sec.

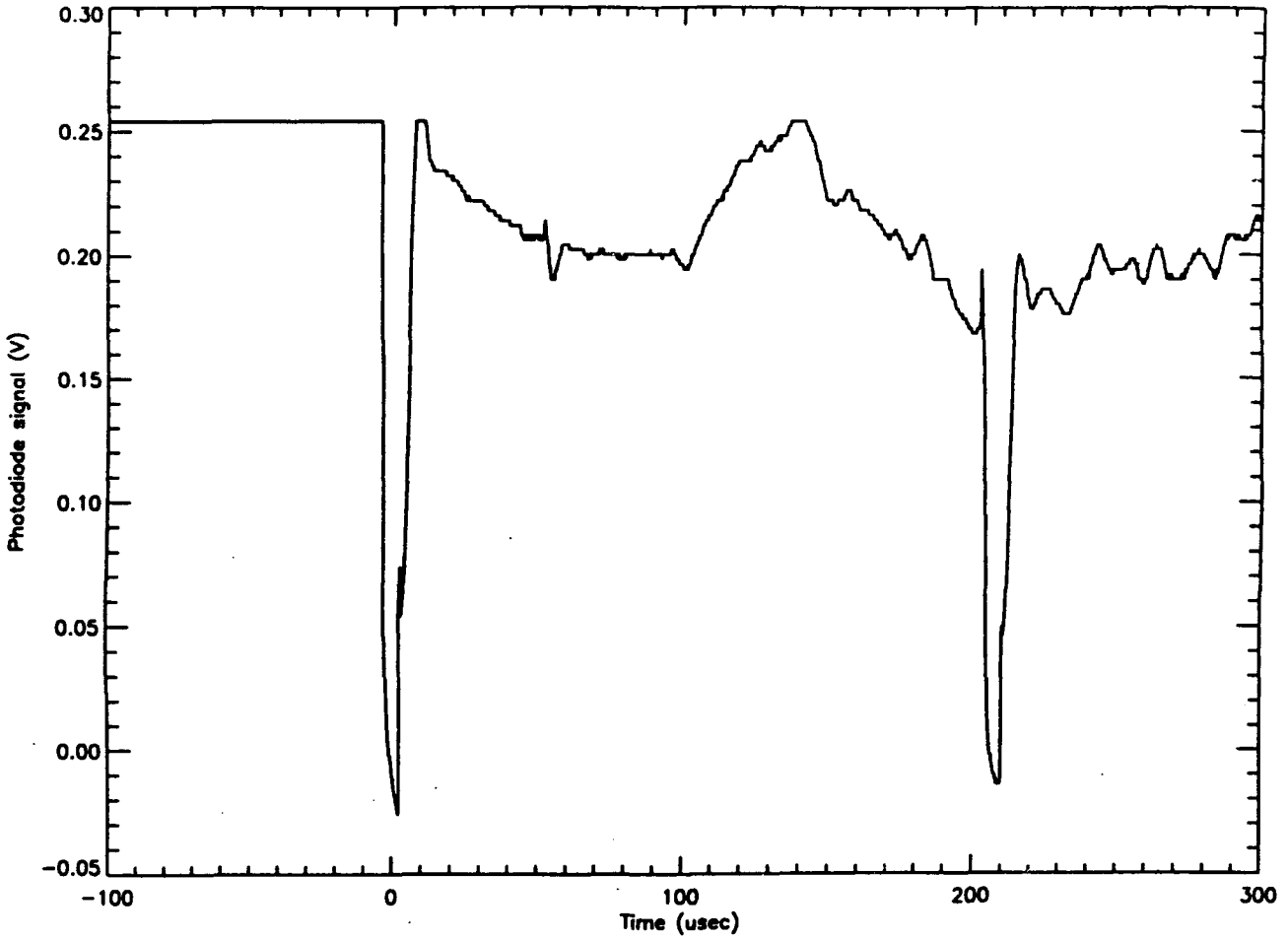

Fig. 2.8 Voltage signals from He-Ne laser in path of TIP projectile. Downward spikes indicate passage of projectile through laser beam at two stations downstream of gun muzzle.

3. SABOT STRIPPING

As in many ballistic research applications, the TIP diagnostic requires a sabot to hold the payload (magneto-optic probe) during acceleration in the gun. This is necessary for several reasons. First, the TIP probes are relatively fragile, and likely would be damaged by sliding contact with the gun barrel. If a refractory enclosure, such as diamond, were used for the probes, this hard material would rapidly damage the barrel wall. Finally, probe geometry is based on the intended function of altering the polarization of light in a plasma magnetic field, and on the constraints of working with optical materials; it would be difficult to manufacture the probes such that a good seal would be made with the barrel walls. In particular, it is convenient to fabricate the probes with a rectangular, rather than circular shape.

Lexan was chosen as a sabot material because of its toughness, light weight, and easy machinability. For the tests carried out in this program, the sabots are single-piece, 30-caliber slugs, having circular holes to accommodate the probes, and with Bridgeman seals machined in the back side to make a good seal in the barrel. The sabot mass is typically 0.7 grams.

Because the sabot material would "poison" the plasmas to which TIP is intended to be applied, the sabot must be separated from the probe prior to the probe's entry into a plasma, and sabot material must be blocked upstream of the plasma chamber. Two sabot-stripping schemes have been explored during this program for integrating the TIP gun with a plasma experiment vacuum chamber. The goal is to fire a stripped TIP probe into a chamber without significant probe wobble or degradation of the base vacuum. The stripping designs that were examined are described below. The need for redesign and extensive testing to get the two-stage light gas gun to operate reliably with helium, precluded carrying out tests of the sabot-stripping schemes.

3.1 Axial Sabot Stripping

The first and easiest to build sabot-stripping scheme is an "axial-stripper", illustrated in Fig. 3.1. The sabot would be a single piece of lexan. When the sabot reaches the end of the barrel it encounters the sabot stripper which has a discontinuity or step in diameter. Upon contact with the step the sabot will decelerate, while the probe, which is free to slide forward in the sabot, will continue forward. The TIP probe will then pass through a hole with a diameter smaller than the sabot diameter. After the

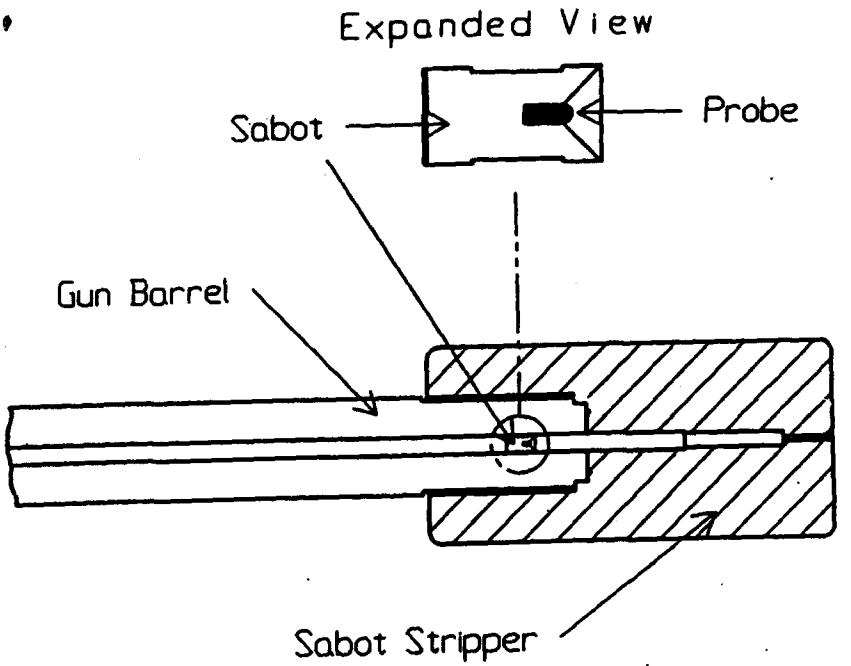

Fig. 3.1 Schematic of axial sabot stripping concept for TIP.

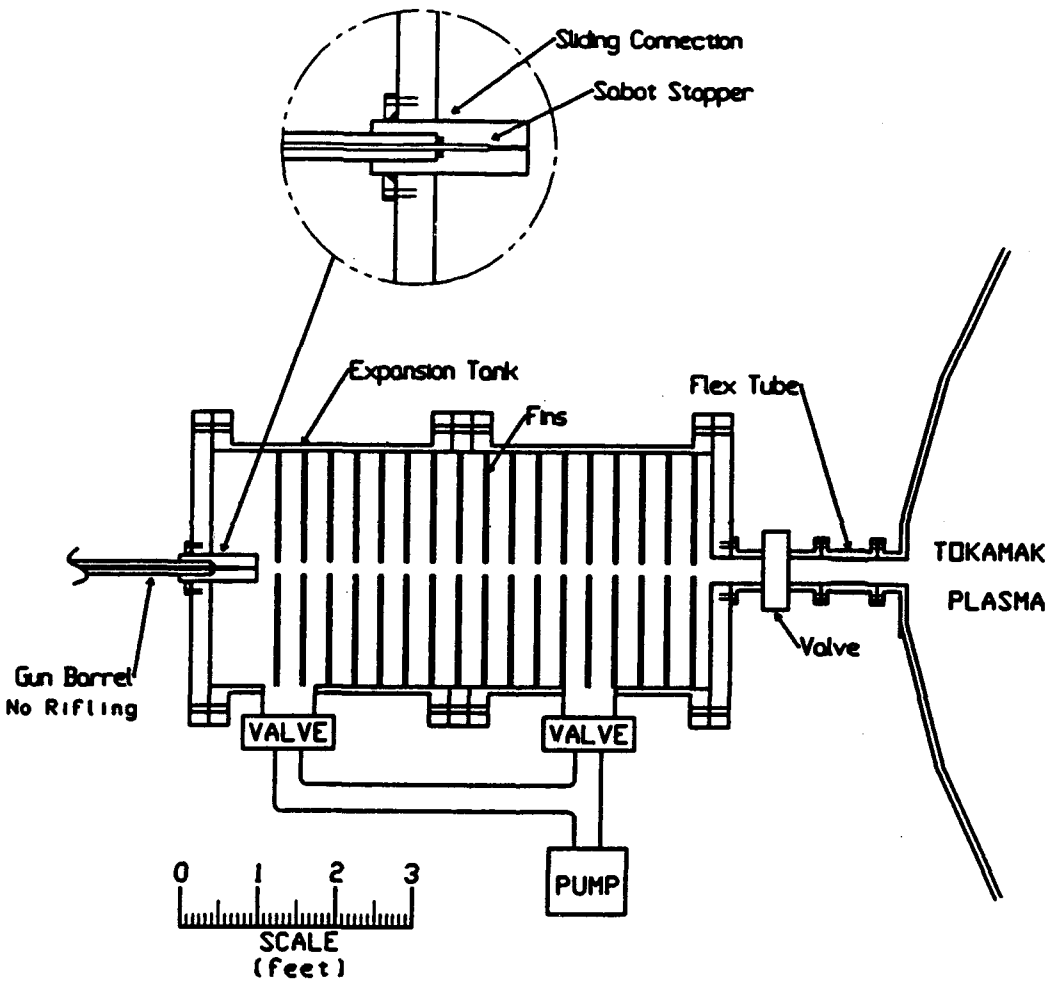

Fig. 3.2 Vacuum interface for axial sabot stripping scheme.

stripper, the probe passes through the vacuum interface shown in Fig. 3.2 to the plasma machine. This vacuum interface consists of a large vacuum tank with baffles installed to inhibit any gas that might leak around the sabot from getting into the experiment before a gate valve can be closed. The sabot stripper is connected to the vacuum tank with a sliding O-ring seal with enables the gun to slide with respect to the tank. In this way the recoil of the gun will not be transferred through the tank to the plasma device. With this first sabot stripping scheme, the barrel need not be rifled or vented, and the sabot has a very simple design which makes the system easy to fabricate.

3.2 Radial Sabot Stripping

The second sabot-stripping technique considered entails the use of a rifled and vented barrel, and the sabot must have a more complicated design. This technique, "radial stripping", is illustrated in Fig. 3.3. The sabot would be made of an obturator, which seals the sabot, and two to four petals that support the projectile during travel down the barrel. Because of the spin imparted to the projectile in the rifled barrel, the petals radially separate from the probe by centrifugal forces when the projectile emerges from the muzzle. The TIP probe then travels through a hole in a plate that is made from a material that is easily cratered, while the petals impact the plate circumferentially to the hole. Cratering of the plate by the impacting petals swages the probe hole shut, preventing the obturator or acceleration gases from passing into the plasma device. Gas expansion slots are cut into the bun barrel just upstream of the muzzle to vent most of the acceleration gas. Venting is needed to minimize the effects of reverse flow, where the energetic gas emerging from the muzzle overtakes the probe and sabot pieces, disrupting the separation process. This radial stripping scheme has operated reliably in previous ballistic research efforts.[9]

A vacuum interface design for the radial stripping scheme is shown in Fig. 3.4. This scheme uses two vacuum tanks, one to capture vented gas from the end of the barrel, and the other to decelerate any gun gases that emerge from the probe hole prior to swaging. The sabot stripper, which is attached to the gun muzzle, passes through a hole in the second vacuum tank which is sealed with a sliding O-ring seal to prevent transmission of gun recoil to the plasma device.

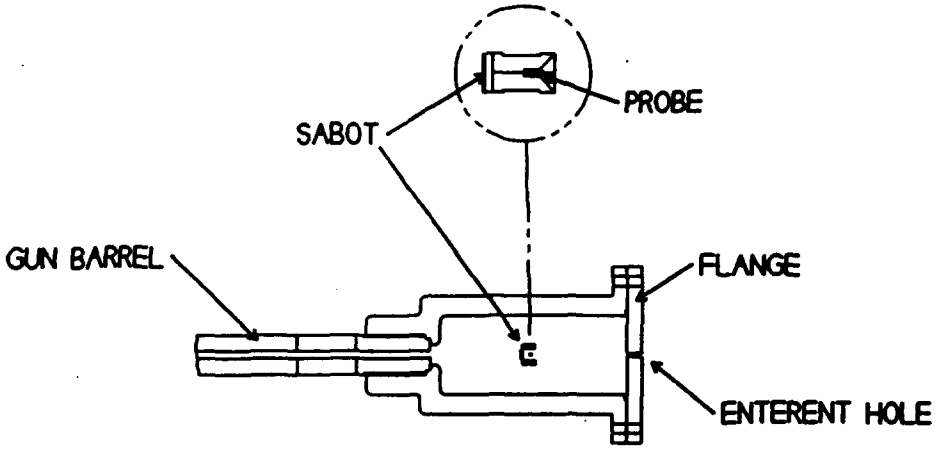

Sabot leaves gun barrel and begins to separate

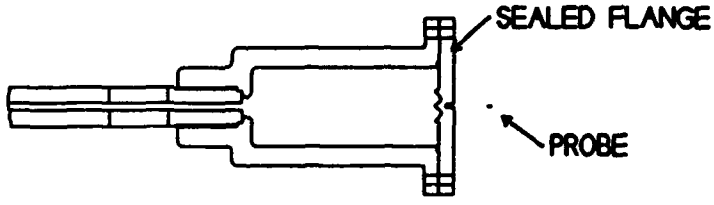

Probe passes through flange and separated sabot swages it shut

Fig. 3.3 Schematic of radial (spin) sabot-stripping scheme..

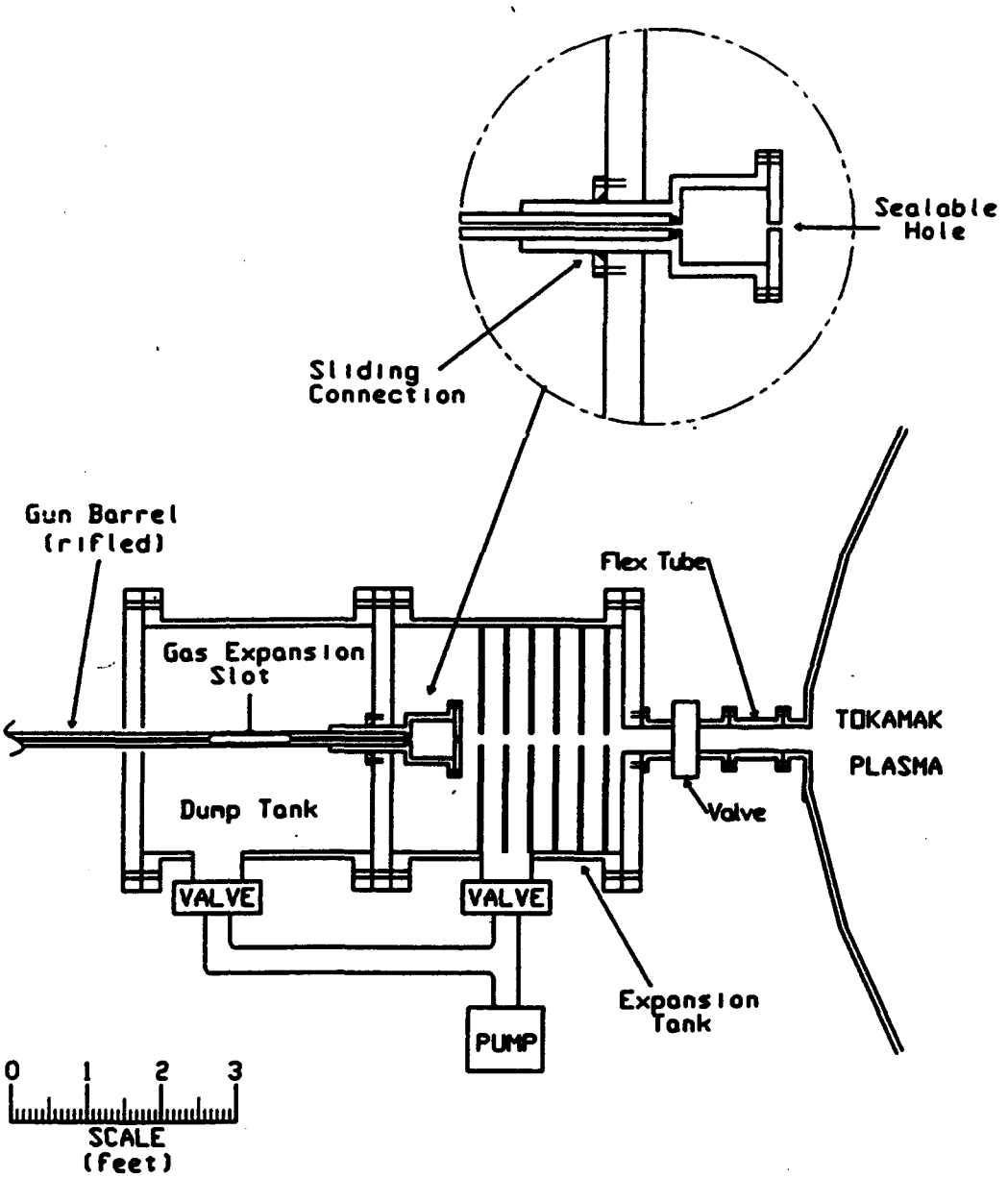

Fig. 3.4 Vacuum interface for radial sabot-stripping scheme.

4. POLARIMETRY DETECTION SYSTEM AND TIP PROBES

The basis for magnetic field measurement in the TIP diagnostic is the rotation of polarization of radiation passing through a magneto-optic material in the presence of a magnetic field. The rotation angle is proportional to B-field strength and probe length. In order to minimize gun requirements, interference with the plasma device, and to achieve good spatial resolution of the field, it is desirable to keep the probe as small as possible. Therefore, accurate field measurements require that the detection system for the retroreflected light from the probe be capable of resolving the polarization to high accuracy. Use of stationary magneto-optic probes for B-field measurements in plasmas has employed polarimetry detection designs with polarization angle sensitivities below 1°. Similar, sub-degree resolution was a goal of the polarimetry system for TIP, and section 4.1 describes the theory of operation, construction and testing of a system that can resolve the polarization to 0.25°. A more detailed description of the system is presented in Ref. 6. Section 4.2 describes the fabrication and characteristics of Faraday probes for TIP measurements, and Section 4.3 discusses results of dropping experiments, where moving probes were used to determine the spatial profile of a static magnetic field. These experiments give results in good agreement with stationary, Hall probe measurements and validate the TIP concept.

4.1 Polarimetry System

4.1.1 Theory of measurement.

The purpose of the electrical detection system is to measure the polarization angle rotation, due to the Faraday effect, by measuring the change in intensity of the incident light on optical detectors. This requires a relationship between the polarization angle, Ψ, and the amplitude of the wave. This is given by

$$|E_{rot}|=E_0 cos\Psi$$

Converting this to power

$$P = E_o^2 \cos^2 \Psi$$

Ideally this could be determined directly by comparing the reduction in signal to a signal from a known polarization angle. However, other factors affect the amplitude of the incoming signal, specifically, wave attenuation and background light sources. Taking these factors in to account with a scaling factor, C, and offset Σ, the power equation then becomes

$$P = C \cos^2 \Psi + \Sigma$$

Having three unknowns requires three equations to be solved simultaneously for the variables Ψ, C, and Σ. Three detectors, with polarizing filters at different angles, provide the necessary three equations:

$$P_o = C \cos^2(\Psi - \alpha_o) + \Sigma$$
$$P_1 = C \cos^2(\Psi - \alpha_1) + \Sigma$$
$$P_2 = \cos^2(\Psi - \alpha_2) + \Sigma$$

If the three polarizing filters are set at equal angles of $\alpha = 60°$, the equations become:

$$P_o = C \cos^2 \Psi + \Sigma = \frac{C}{2}(\cos 2\Psi + 1) + \Sigma$$

$$P_1 = C \cos^2\left(\Psi - \frac{\pi}{3}\right) + \Sigma = \frac{C}{2}\left(-\frac{1}{2}\cos 2\Psi + \frac{\sqrt{3}}{2}\sin 2\Psi + 1\right) + \Sigma$$

$$P_2 = C \cos^2\left(\Psi - \frac{2\pi}{3}\right) + \Sigma = \frac{C}{2}\left(-\frac{1}{2}\cos 2\Psi - \frac{\sqrt{3}}{2}\sin 2\Psi + 1\right) + \Sigma$$

These equations are solved using a least-squares minimization of the quantity R, where R is given by

$$R = \left\{\frac{C}{2}(\cos 2\Psi + 1) + \Sigma - P_o\right\}^2 + \left\{\frac{C}{2}\left(-\frac{1}{2}\cos 2\Psi + \frac{\sqrt{3}}{2}\sin 2\Psi + 1\right) + \Sigma - P_1\right\}^2 + \left\{\frac{C}{2}\left(-\frac{1}{2}\cos 2\Psi - \frac{\sqrt{3}}{2}\sin 2\Psi + 1\right) + \Sigma - P_2\right\}^2$$

The R minimization, $(dR/d\Psi = 0)$, results in an expression for the polarization angle Ψ:

$$\tan 2\Psi = \left\{ \frac{\sqrt{3}(P_1 - P_0)}{2P_0 - P_1 - P_2} \right\}$$

This result for Ψ is valid only at equal $\alpha = 60°$ angles.

4.1.2 Calibration and polarization angle calculation

In general, the detector polarizing filters will not be at equal $\alpha = 60°$ angles. To more accurately measure the angle of polarization, this can be accounted for in the calculations by considering the case of arbitrary angles, where the solution is found from a converging iterative analysis from the ideal case where $\alpha = 60°$ equal angles.

For arbitrary angles, the offset and scaling terms do not simply cancel. To solve this using an iterating method the system must be calibrated. The individual detector power equations are written as

$$S_i = A_i I_0 + b_i P \cos^2(\Psi - \alpha_i)$$

where $A_i I_0$ represents the offset due to background unpolarized light, and $b_i P$ represents the scaling factor. An unpolarized light source, I_0 is applied to the detectors. Solving for A_i:

$$A_i = \frac{S_i}{I_i}$$

A_i is then normalized such that $\sum_i A_i = 3$. A known source of polarized light is then applied to the detectors. By varying the polarization angle, b_i and α_i can be determined by solving simultaneous equations involving only b_i and α_i.

Once calibrated, the problem is solved for arbitrary angles using an iterating method and the least squares approach. The values for the coefficients are written as equations of summations. Assuming the initial condition of α_i being $60°$ apart, an initial value of Ψ can be obtained using only the measured values S_i as was previously shown. Taking this value of Ψ

and substituting into the equations for I and P, a new value of Ψ is obtained. This is iterated until $\Delta\Psi$ between iterations is acceptably small. The magnitude of the magnetic field is then determined by

$$B = 2LV(\Psi - \Psi_0) \qquad (1)$$

where L is the length of the Verdet material, V is the Verdet coefficient, and Ψ-Ψ_0 is the measured change in the polarization angle after a double pass in the probe.

4.1.3 Description of polarimeter

A schematic of the polarimetry system is given in Fig. 4.1 and photographs of the system are shown in Fig. 4.2. The system is on two levels, with the 632 nm He-Ne illuminating laser on the lower level. The laser beam passes through a beam expander formed from a pair of lenses, and a mirror reflects the light to the upper level of the system.

The upper level consists of a beam splitter, a combined lens and filter, two additional beam splitters to direct the light to 3 discrete detectors. As the beam impinges on the first beam splitter, it is directed towards the probe, which retroreflects it back to the splitter. The return beam then passes through a focusing lens and a narrow-band (10 nm) filter passing the 632-nm wavelength. The beam is then split into two oblique beams beam splitters, and the remaining light passes to the third detector. In front of each detector is a polarizing filter, and the three polarizers are offset by 60° as described above. The spacings between optical components were chosen such that incident angles on optical components and overall size remain small to minimize measurement errors. Dimensions for the total system, including a protective beam dump enclosure, are 75-cm long, 25-cm high, and 30-cm high.

The system support components have been designed to allow position adjustment in every plane of motion while minimizing the overall size of the system. The desire to minimize size was based on reducing the impact of this system on the space surrounding a plasma machine. The resulting design height which accommodated each component is 7.5 cm from the surface to the center line of the beam. All components on the lower level are mounted on a single track with carriages designed to allow motion along the direction of the beam only. All components on the upper level are mounted on a similar track, with exception of the two angled detectors.

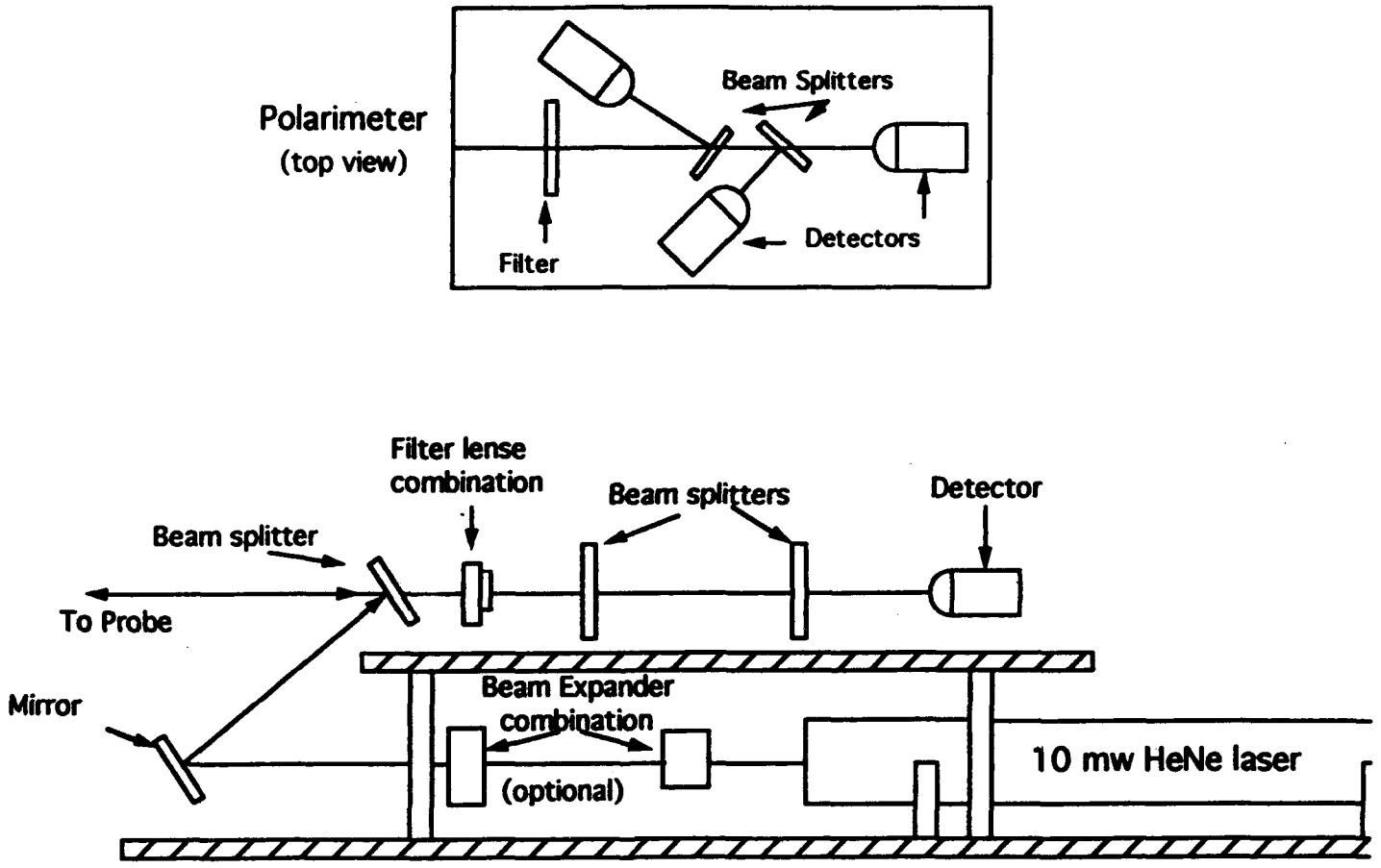

Fig. 4.1 Schematic of TIP polarimetry system.

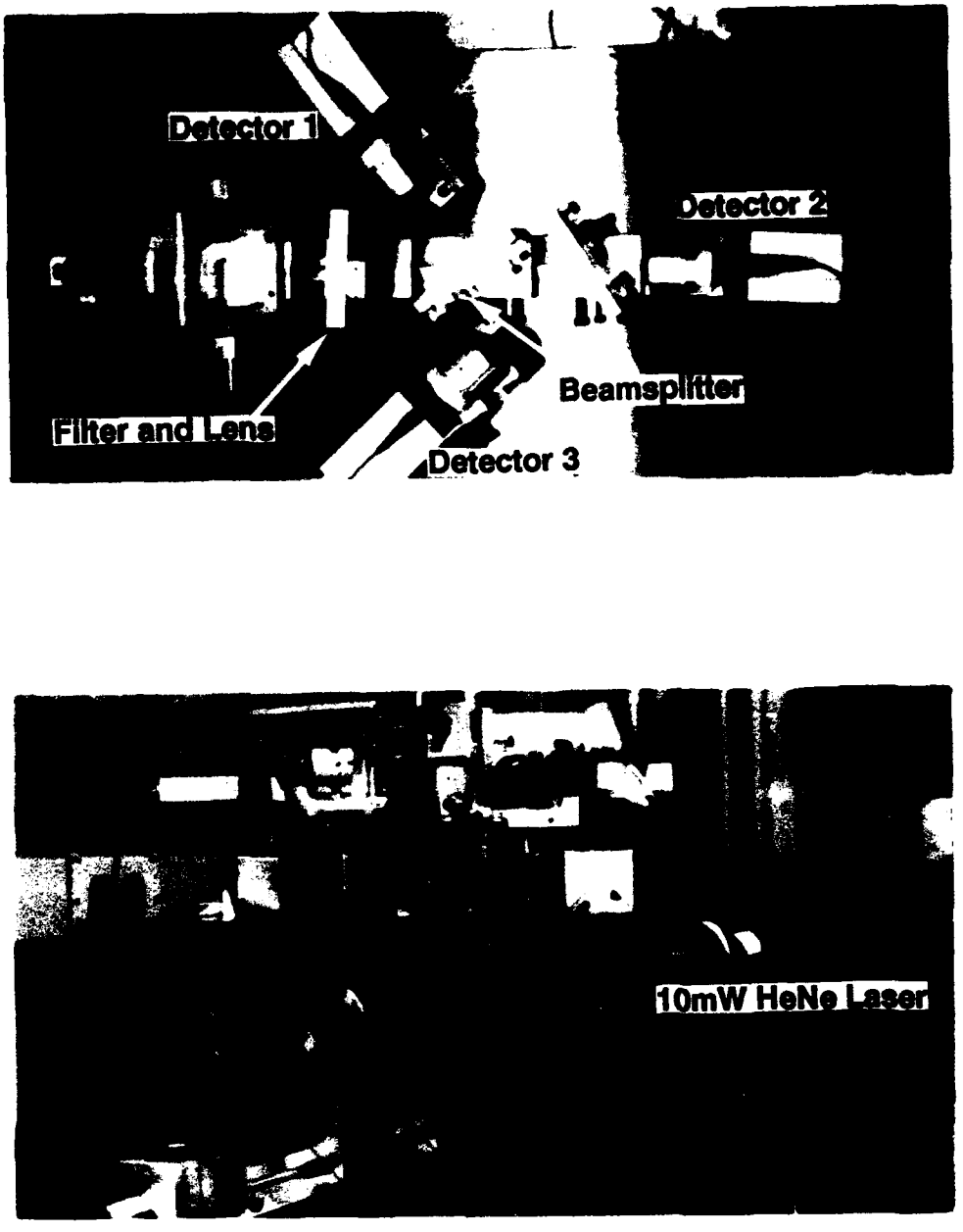

Fig. 4.2 Photograph of TIP polarimetry system.

These are mounted on separate tracks with their respective filters. Once aligned, the entire system will be enclosed with a removable cover to minimize background light.

The three photodetector assemblies have been engineered to allow the polarizing filter to be rotated as required for initial calibration, while maintaining the focal point of the lens precisely on the surface of the photodiode. Each polarizer is cemented with optical cement directly to a lens that images the return beam to a small spot on the 2-mm square detector surface. The lens/polarizer can easily be rotated to calibrate the polarization separately for each detector, without affecting the imaging of the lens onto the detector.

4.1.4 Calibration of polarimeter

The polarimeter was calibrated in a manner that corrects for the non-ideal behavior of the beam splitters. To calibrate, laser light is directed incident to the polarimeter and the polarization angle is varied. Fig. 4.3 shows the response of the three photodetectors together with a functional $\cos^2$ fit. Ideally, the responses from the detectors should follow this fit exactly. In practice, the non-ideal separation of the s- and p- polarization components creates the systematic departures seen in Fig. 4.3 as the linearly polarized light becomes partially elliptic. To correct for this effect, the calibration curves are fit using a least-square minimization to a 9th degree polynomial. These functional fits, shown in Fig. 4.4, then describe a one-to-one correspondence between the detector voltages and the polarization angle. To determine the polarization, the three photodetector signals are measured and a least-square fit is calculated for the difference between the measured quantities and the calibration fits. Although a least-square method is used to simplify the analysis, the solution is well-defined since there are three signals and three unknowns (intensity, background, and polarization angle.)

Once the polarization angle of the retroreflected laser light is determined, the local magnetic field at the position of the probe is given by Eq. 1. The product LV in Eq. 1 is a constant, determined by an independent calibration where the response of the TIP probe is compared to that of a Hall Probe.

4.2 Probe Fabrication

Faraday-rotator magnetic field probes have been constructed using both Terbium-doped borosilicate glass (FR-5) and Manganese-doped Cadmium Telluride,

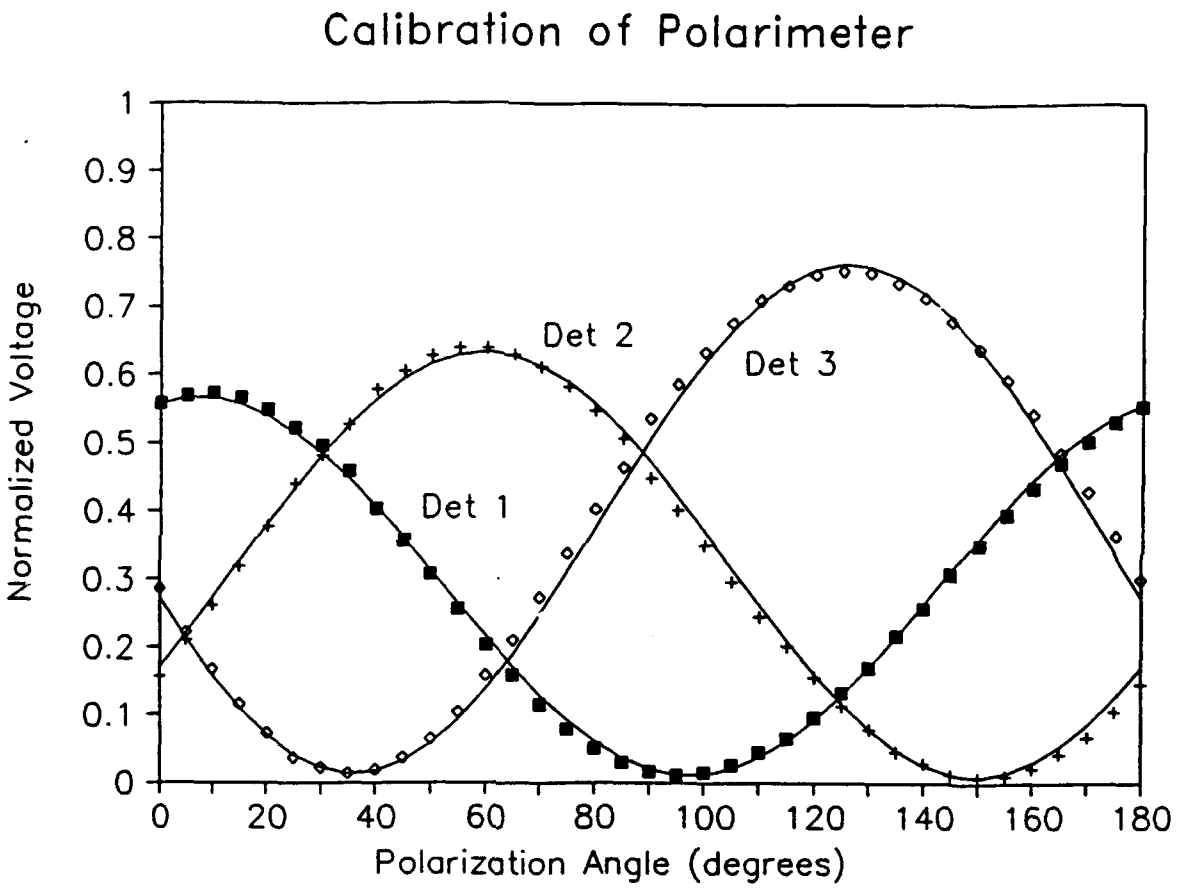

Fig. 4.3 Calibration signals for TIP polarimeter. Solid curves are cos^2 fit.

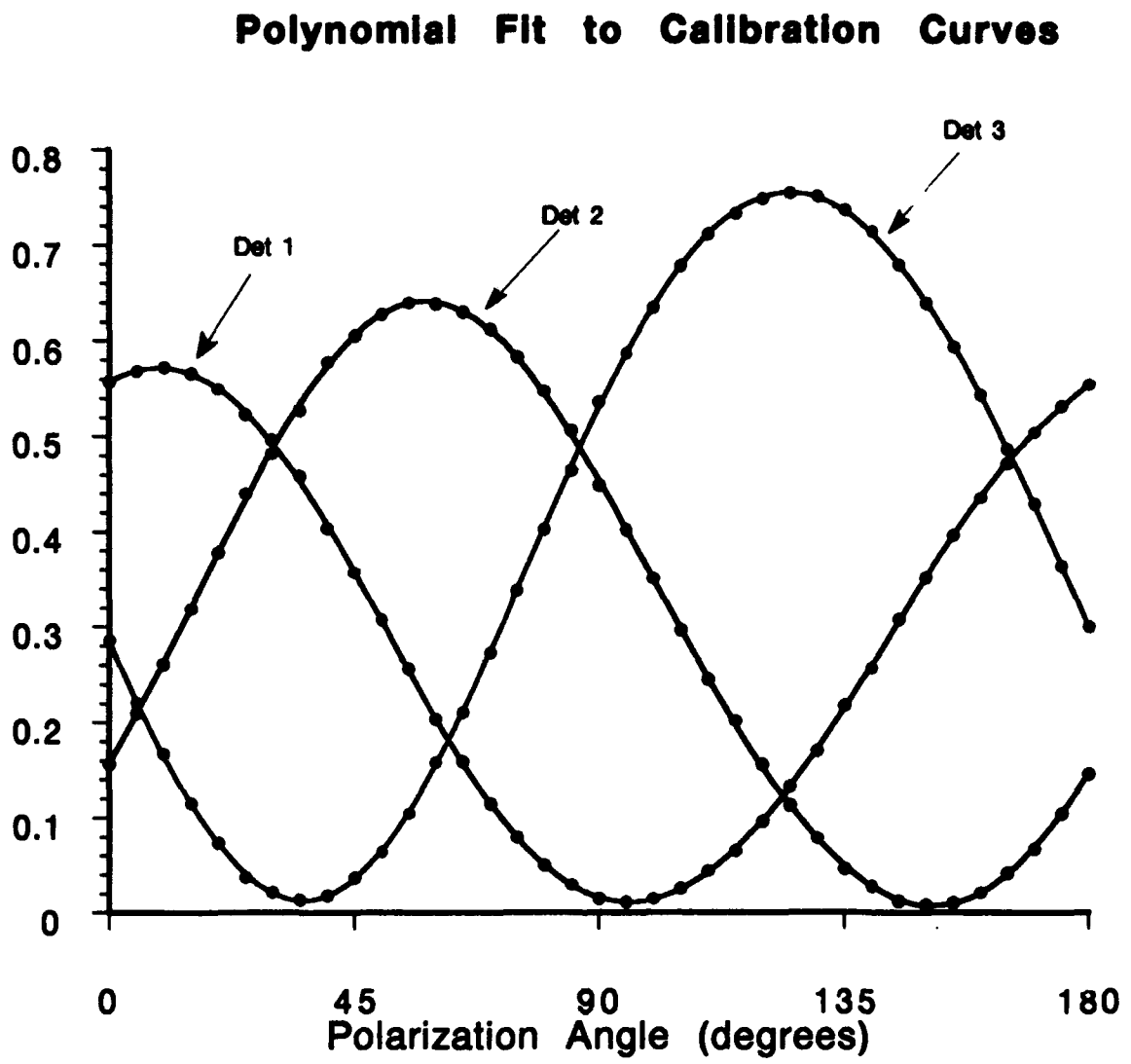

Fig. 4.4 Calibration curves for the TIP polarimeter using a 9th degree polynomial fit.

with corner-cube retroreflectors and with sheet retroreflectors. Fig. 4.5 shows a photograph of the two probe materials and retroreflectors.

The FR-5 glass material used in the dropping experiments has a Verdet coefficient of 0.00413 degree/G-cm at the 628 nm wavelength of the He-Ne laser. Retroreflection was accomplished using an aluminized, 3-mm-diameter corner-cube attached to the rear of the probe. Initial FR-5 probes were easily fabricated using equipment at the Harris Hydraulics Laboratory on campus. After testing, probes of suitable dimensions were ordered from the FR-5 supplier.

We also constructed probes from CdMnTe material. The higher Verdet coefficient of this material results in a sensitivity that is 40 times that of the FR-5 glass. However, fabricating probes from CdMnTe proved to be difficult since the material easily chips and cracks. Probes that were constructed proved to have poor optical quality due to internal faults thought to arise from the material being grown as polycrystalline. A commercial supplier was found and CdMnTe probes were fabricated to TIP probe specifications.

Transmission and reflection measurements performed on various thicknesses of CdMnTe material showed that the reflectivity was approximately 32%, somewhat higher than expected based on the refractive index of 3.0 for this material. The anomalously high reflection is thought to be due to surface defects. For a double-pass TIP probe, as much as 95% of the original laser intensity can be reflected from the four interfaces. Since loss of intensity in the TIP diagnostic can in principle be offset by supplying more light from the laser, this loss of intensity is not a fundamental limitation. However, the detection of light reflected from the probe surfaces poses a very serious problem, since it can easily swamp the Faraday-rotated light of interest, which is at much lower intensity. This difficulty made it impossible to obtain meaningful results when CdMnTe material was used for the dropping experiments. Attempts to improve performance by applying antireflection coatings were only marginally successful, since it was found that the CdMnTe material has intrinsic birefringence and crystal defects that compete with the Faraday rotation effect sought. For these reasons, despite the very high sensitivity of CdMnTe as a TIP probe, its use was discontinued for TIP.

The low refractive index of FR-5 glass (n=1.7) results in a front-face reflection of 6.7% and a double-pass transmission of 57%. The front-face reflection did not prove to be a problem for magnetic field measurements described below.

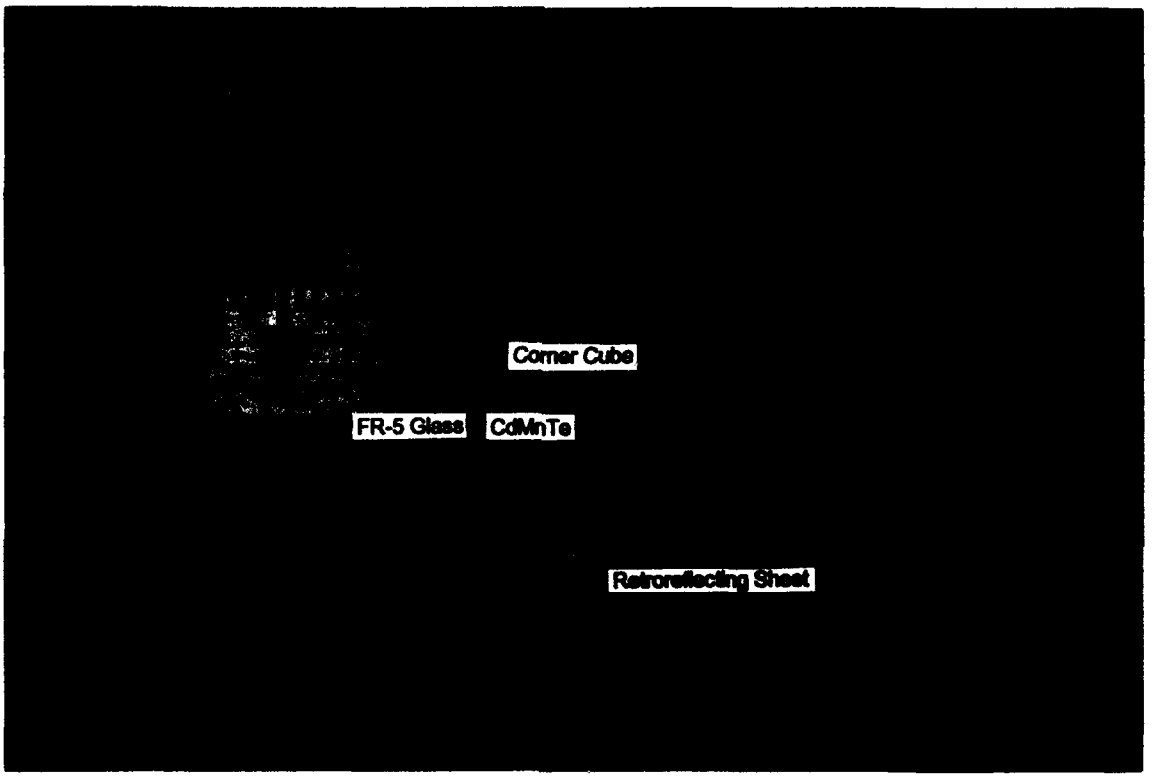

Fig. 4..5 Photograph of TIP probe Verdet materials CdMnTe and FR-5 glass. Also shown is a corner cube retroreflector and retroreflecting sheet material.

Subsequent to the measurements of magnetic fields carried out using an FR-5 probe and corner-cube reflector, tests were conducted on the performance of retroreflecting sheet material. The use of this material is advantageous because it allow for a more compact and lightweight design. The measurements indicated that little absorption or scattering occurred for the sheet, but that the return light was spread over a full angle of about 2.5°, due to the non-ideality of the micro-prism retroreflectors on the sheet. This spread will diminish the detector signals of the polarimeter, although higher laser intensities can be used to offset this. The divergence might actually be somewhat useful, in that the return signals might be less affected by any pitching motion of the probe.

4.3 Magnetic Field Measurements Using a Moving Probe

To demonstrate the ability to track a moving probe and to accurately measure the change in polarization angle, a TIP probe was dropped through a permanent magnet and the polarimetry system was used to measure the local magnetic field. The experimental arrangement for this test is shown in Fig. 4.6. By performing many drops and comparing the spread in the polarimetry system response, we were able to determine the accuracy of the system. The probe used for this experiment was a 4-mm-square, 8-mm-long, sample of FR-5, with a corner-cube retroreflector attached to the rear face. The probe assembly is illustrated in Fig. 4.7.

Fig 4.8 shows the raw data from the drop experiment where the intensity of each of the three detectors is plotted vs time. The effects of the magnetic field are seen as a small bump shortly after 50 msec, riding on the large amplitude change in intensity due to probe position and imaging. The data is analyzed as described above to yield the magnetic field vs position as shown in Fig. 4.9. The TIP measurement is seen to agree well with magnetic field measurements using a Hall probe that was passed through the magnet. The average probe velocity during the drop was 2.3 m/sec. Here, the TIP measurement as a function of time has been converted to position using velocity measurements made from laser-photodiode pairs directed across the path of the probe. Due to the low field strength of the permanent magnets, the maximum polarization angle change during the drop is 12°. In spite of the small Faraday rotation in this field, good measurement resolution is seen, especially near the coil ends, where the same low-magnitude field asymmetries are seen by both the TIP and Hall probes.

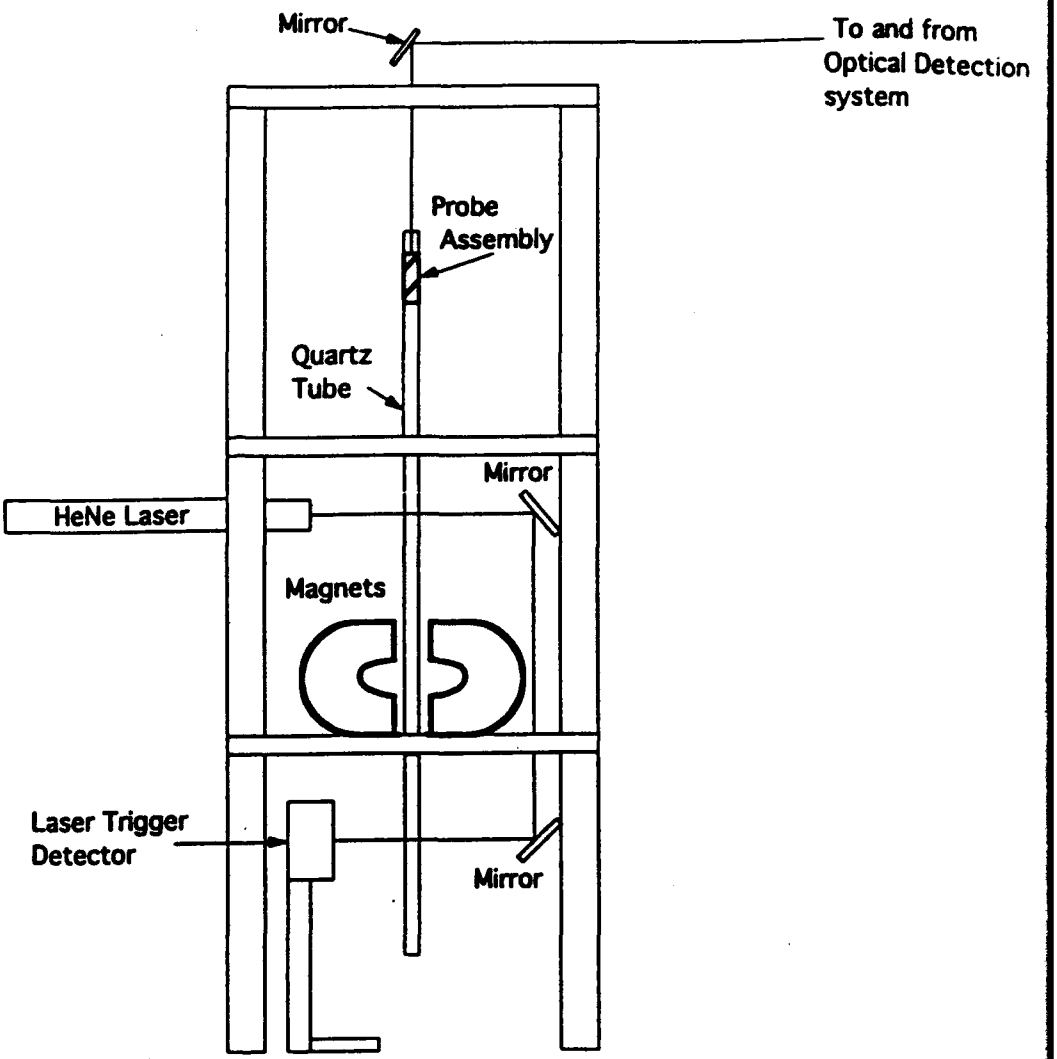

Fig. 4.6 Schematic of TIP validation experiment. FR-5 TIP probe is dropped through a quartz tube passing through field of a fixed magnet. Field determination from the rotation of retroreflected light from moving probe agrees with static Hall probe measurement.

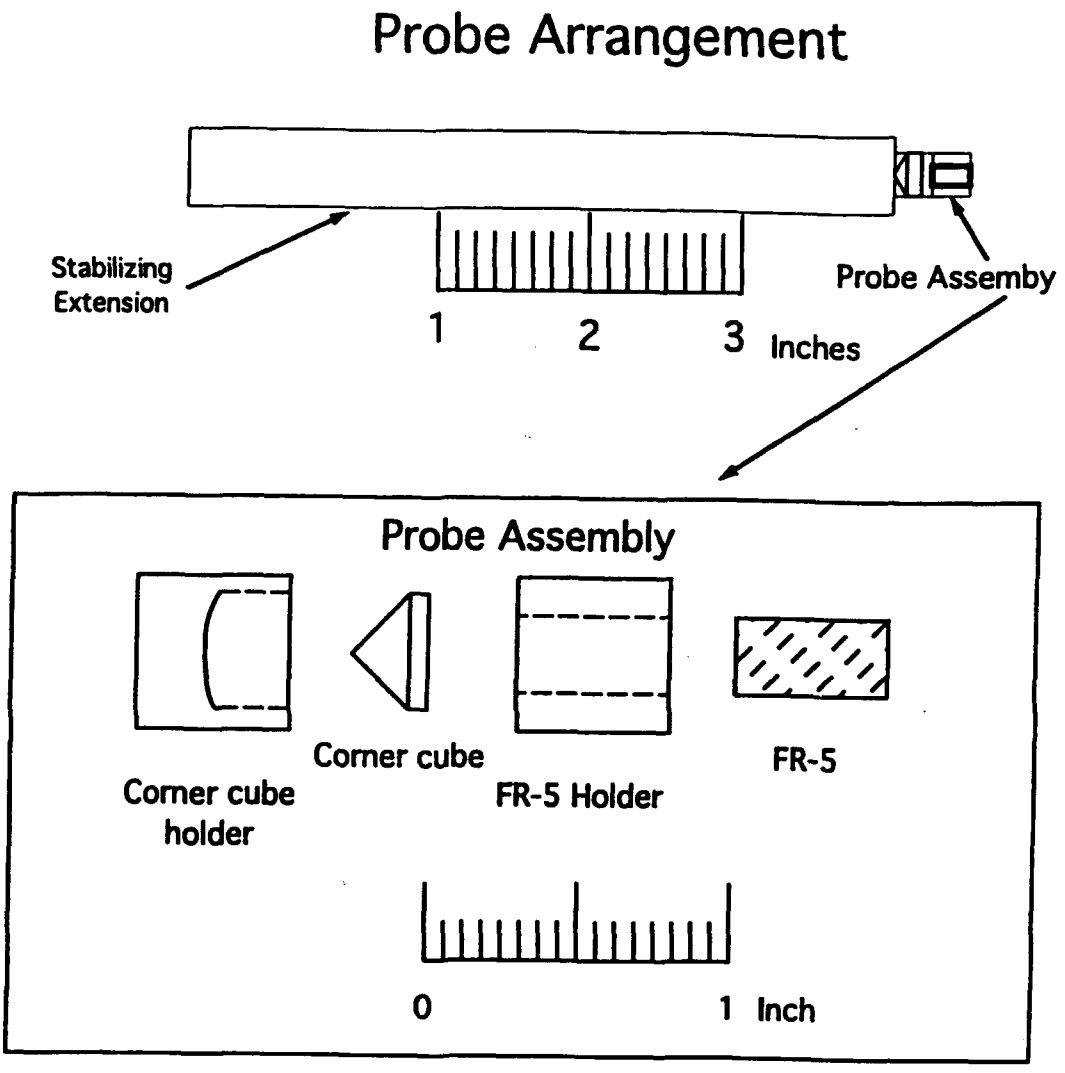

Fig. 4.7 Probe assembly used for the TIP dropping experiment. The FR-5 probe and corner cube are held in place by a polyethylene shell.

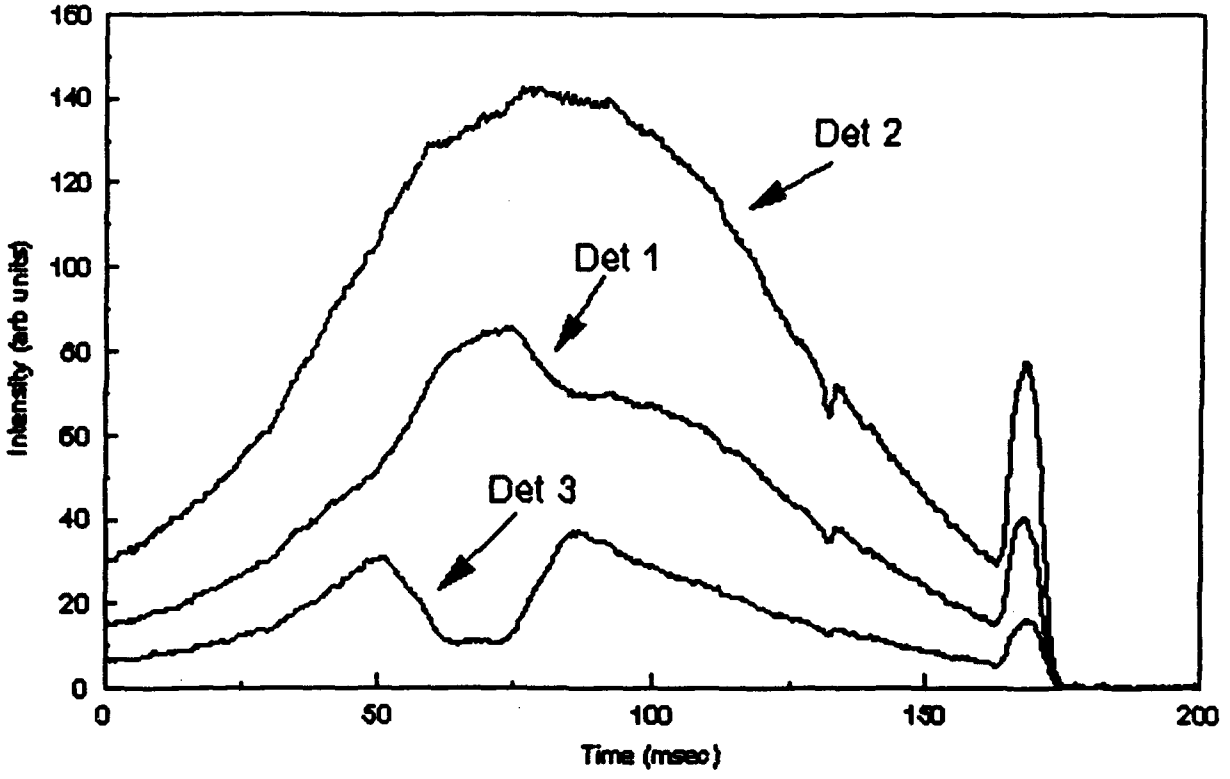

Fig. 4.8 Detector signals from TIP dropping experiment. Detector polarizers differ by 60°.

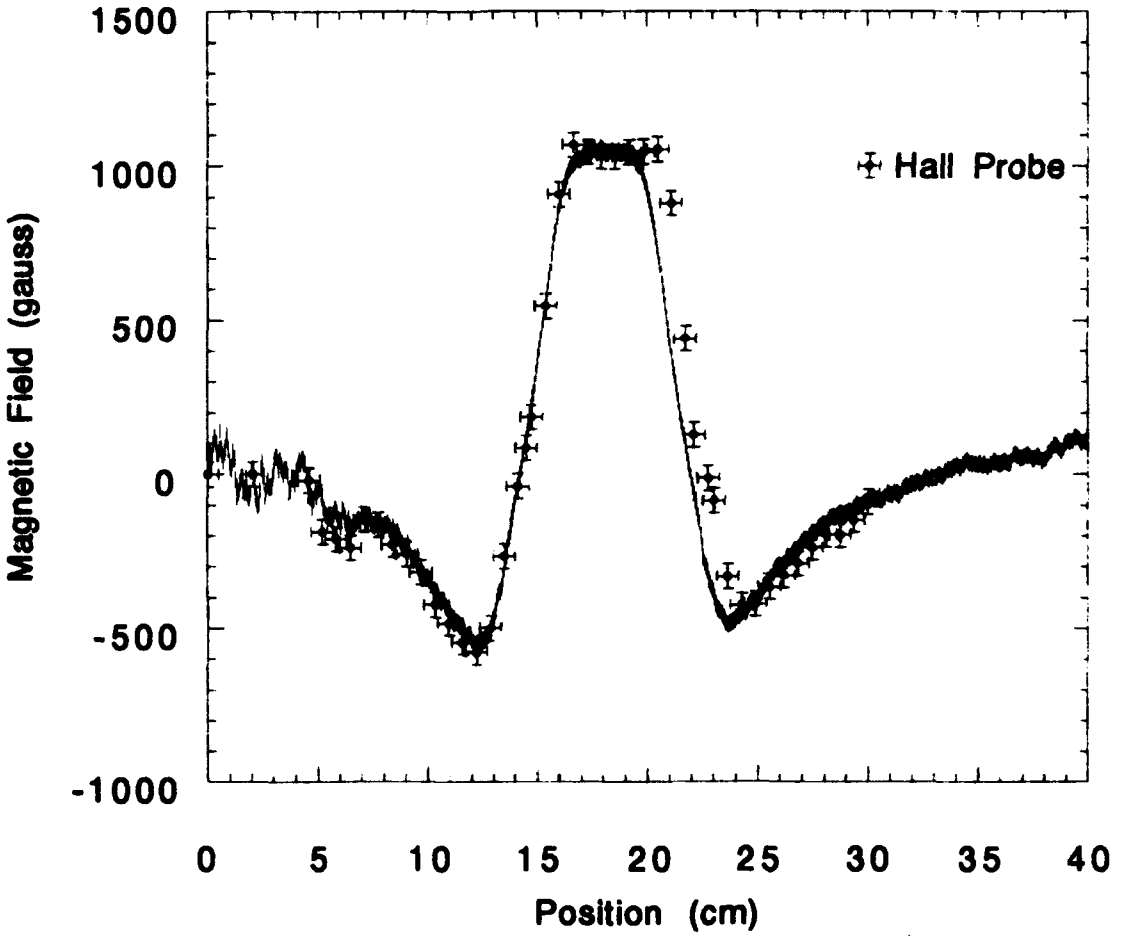

Fig. 4.9 Magnetic field as a function of position as determined via TIP dropping experiment (dotted line) and by static Hall probe measurements (crosses).

The field strength error bars for the TIP measurement correspond to the maximum range seen from several separate drops and give an average error of ±40 G. This corresponds to a polarization angle resolution of 0.25°. The polarization angle error can be further reduced using digitizers more accurate than the 8-bit ones used.

The angular resolution of our polarimeter is comparable to that of other, more complicated polarimetry systems. For example, the polarimeter used for the Motional Stark Effect (MSE) diagnostic on PBX-M has an uncertainty of 0.5°.[10] The polarimeter used for the MSE diagnostic on the DIII-D tokamak has an uncertainty of 0.2°.[11]

These dropping experiments were a valuable confirmation of the applicability of the TIP concept as well as a test of the polarimetry system. The ability to track a moving projectile with a retroreflected laser beam was demonstrated, and despite wide variation in return light intensity, the magnetic field could be accurately determined. Smaller intensity fluctuations are expected for the return light from a gun-launched probe, because of the longer imaging distance.

5 CARBON/DIAMOND ABLATION TESTS IN A HOT PLASMA

5.1 Introduction

In order to conduct preliminary tests of Diamond versus Carbon pellet ablation in an actual plasma, a prototype pellet injector was constructed and taken to the University of Wisconsin, in Madison, Wisconsin. There 0.6 mm laser-cut cylindrical diamonds (and/or graphite cylinders) were launched at 400-500 m/sec into the Madison Symmetric Torus (MST) reversed field pinch, a large plasma device with an energetic, long-lived plasma. Substantial differences, seen photographically, between the diamond and carbon pellet tracks indicate a significantly reduced ablation rate for the diamond pellets. For reference purposes, similar size frozen hydrogen pellets were also launched into the same plasma.

5.2 Compact Light-Gas Gun Injector

A simple sliding-breech loader mechanism was constructed to allow up to 0.6 mm diameter pellets to be inserted into firing position, in front of a fast opening (and closing) hydrogen gas valve, which then accelerates the pellet down a 30 cm long stainless steel barrel. A $1\,cm^3$ hydrogen gas reservoir at a fill pressure of 1100 psi provides the gas pulse, which is focussed (in a non-optimized manner) onto the pellet. The gas pulse is applied over a 100-200

μsec period by the opening and closing of an electromagnetically-driven, fast-acting, patented Los Alamos fast gas puff valve. The valve technology was originally developed in the CTR-3 plasma group for application on end-plug fuelling of a linear theta-pinch in 1979, and a US patent #4344449, Aug. 17, 1982, was issued to Jim Meyer of Los Alamos. We have obtained one valve and spare parts from LANL. The completed injector and the box of seven diamond pellets are shown in Fig. 5.1. The valve is triggered by a krytron-driven ruby-laser power supply and capacitor, providing a 2.0 kV voltage pulse to a spiral-wound coil in the gas valve, carrying a 6 kA current pulse that causes a magnetic field to accelerate the valve stem, forcing it open. Compression of a nonlinear gas spring returns the valve to its closed position.

Tests of the gun in the open atmosphere, yielded pellets travelling at approximately 300 m/sec. When the gun was integrated with its two-part vacuum system (a low pressure rough pump and surge tank near the barrel, and a high vacuum (turbo-pumped) section isolated by a 2-meter flight tube), the velocity improved to 400-500 m/sec, dependent on the pellet mass. To conserve the number of laser-cut diamonds that were obtained (only seven), all lab bench testing was conducted with metal or graphite pellets, while the system was in Seattle. Pellet velocities were directly measured by observing the timing of interrupted light signals from a He-Ne laser and fast photodiode pairs.

5.3 Pellet/Plasma Test Results

During a two-week period in August 1991, the gun and equipment were installed on the MST device in Wisconsin. The completed installation is shown in Figure 5.2, with four different views of the apparatus, next to the relatively large MST plasma torus. Pumping facilities to remove the unwanted gas load from the light gas gun were provided by the MST group. A four-shot cryogenic hydrogen pellet injector, which was also undergoing initial testing during the same run, was used for the reference hydrogen pellet injection.

After installation of the injector system at Madison, and mounting of appropriate optical monitors (imagery and light diode sensors), the first pellet/plasma shots were conducted using graphite pellets, ranging in length from 0.75 mm to 3.0 mm. A typical 400 m/sec, 2 mm long x 0.6 mm dia. graphite pellet ablation track ablating in a Helium target plasma is shown in Fig. 5.3. The pellet crossed the entire plasma, with little deflection, although it clearly shows fragments breaking away from the main body of the track as it crosses the plasma. These tiny fragments all curve to the right in the picture, due to a rocket-effect caused by differential

ablation of the pellet(s) being bombarded preferentially from the electron drift direction. The bright spot at the top of the photo is due to Helium light emission from a gas puff fuelling valve located on the inner, lower half of the plasma torus, and is not associated with the graphite pellet striking the back wall of the vessel.

As a comparison, two hydrogen pellets, viewed from above and injected at 800 m/sec are shown in Fig. 5.4. The scales are similar to Fig. 5.3, and show an ablation track that is much wider and more diffuse than in the case of carbon (graphite). The pellets also suffered a greater deflection in the electron drift direction, and may have actually struck the bottom of the vacuum vessel.

An important result from this experiment is that launching diamonds is not so easy as graphite, at least in the apparatus used in this test. Seven diamond pellets were attempted, but only two fragmented diamonds were observed entering the plasma. Severe difficulties with the diamond jamming, and evidently breaking (or spallating) in the gun breech were encountered, as the gun was fired. It was noted that the actual size of the diamond cylinders (slightly conically shaped due to the laser-cutting fabrication process) were 0.02 mm larger in diameter than the graphite, while also being shorter than most of the graphite pellets we launched. On some shots the diamonds were actually recovered in the breech mechanism. This was first realized as a scratch when sliding open the bronze/stainless steel breech mechanism, or when the next graphite shot would fail to be seen on the velocity monitor, because it was blocked by a jammed diamond. The use of a sabot, as planned on the TIP experiment, should solve these problems.

The diamonds showed the thinnest ablation track that was observed, compared to hydrogen, lithium, or graphite pellets. A diamond track (corresponding to approximately 30% of the original pellet) from a diamond that made it into the plasma at 400 m/sec is shown in Fig. 5.5. It had a blueish-white tint, and was quite dim, with few signatures on other plasma-related monitors, such a CIII, CIV, or CV emission lines. Unfortunately because the mass of this pellet is unknown, a quantitative comparison cannot be made, although the diamond impact on other plasma parameters was minimal (to nonexistent). During this run, the plasma density interferometer was not functioning, hence the basic plasma density could only be inferred from bremsstrahlung measurements.

5.3.1 Conclusions of the Diamond Ablation Test

The difficulties encountered injecting diamond pellets supports the design for the TIP projectile, in which the diamond encased probe will be held by a sabot during the acceleration through the two-stage light gas gun. The pellet injector used in the diamond ablation study will be similarly modified to permit reliable diamond injection into the MST plasma.

The qualitative results of the diamond ablation study are very promising. The diamond ablation track is both thinner and emits less light than the ablation tracks from the carbon pellets. When the diamond pellets were injected, no large effects were seen on other plasma related monitors, although at the time of the tests the plasma density interferometry system on MST was not operational.

To obtain a quantitative measurement of the diamond ablation rates, further tests will be conducted when the MST interferometry system is operational.

Fig. 5.1 Single-shot gas gun used for prototype experiments, made at the University of Washington, and used at the University of Wisconsin, including electromagnetic gas valve on left, loading mechanism, and exposed 0.6 mm i.d. barrel. Also in the photo is a pencil and box with seven test diamonds.

Fig. 5.2 (a) Close-up of installed gun, with 7 kA feed cable and high pressure hydrogen line; (b) Light-gas gun mounted on low-pressure surge tank, with high pressure hydrogen gas bottle nearby; (c) "front-end" differentially pumped section, with pellet guide tube entering from left, and plasma torus seen on right, after vacuum cross (for velocity measurement via laser/diode pair) and isolation gate valves; and (d) Photo along installed "beam-line", which isolates the high pressure gas surge from the high vacuum required in the plasma torus.

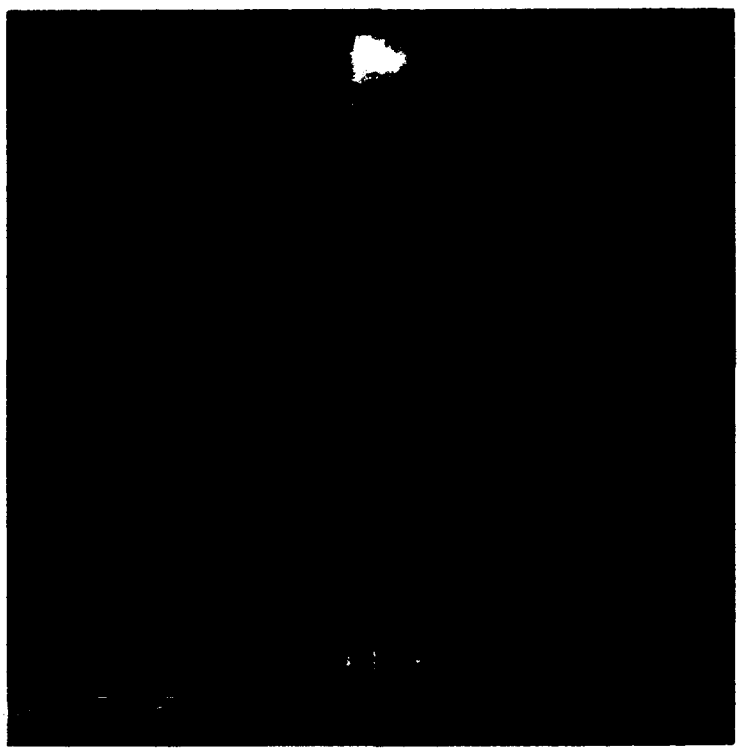

Fig. 5.3 Large Graphite pellet (0.55 mm x 2.0 mm), viewed from above, launched at 400 m/s from the outside midplane of the MST plasma. It fully penetrates the $n_e \sim 10^{13} cm^{-3}, T_e \sim 200 eV$ plasma, while small fragments break off and are accelerated to the right by an asymmetric energy flux causing differential ablation and "rocketing" of the plasma. Curvature of the track is in the electron drift direction.

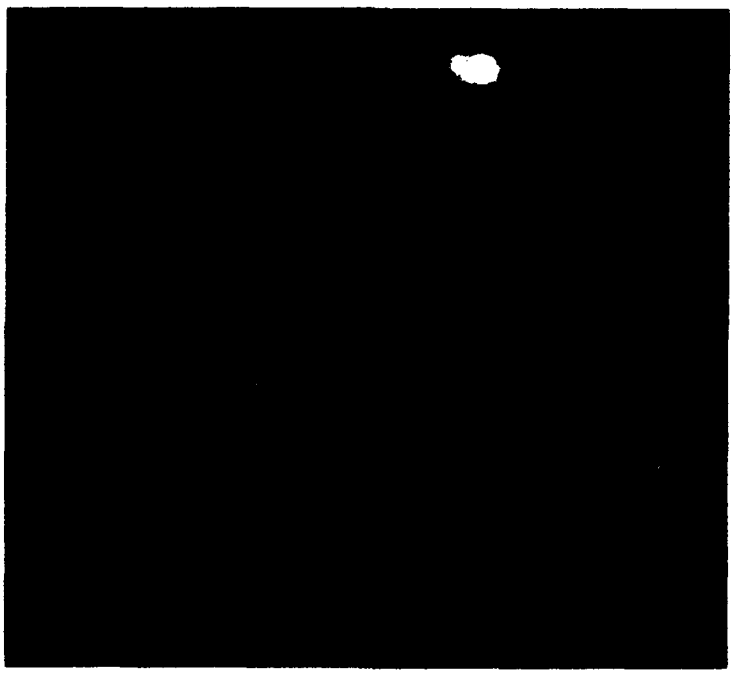

Fig. 5.4 Two hydrogen pellets (each containing $\leq 6 x 10^{19}$ H atoms) are seen crossing ~ $\frac{3}{4}$ of the 1 meter diameter MST plasma. The bright pink spot at the upper right is due to gas puff refueling of the plasma throughout the discharge by a puff valve on the lower inner wall of the torus.

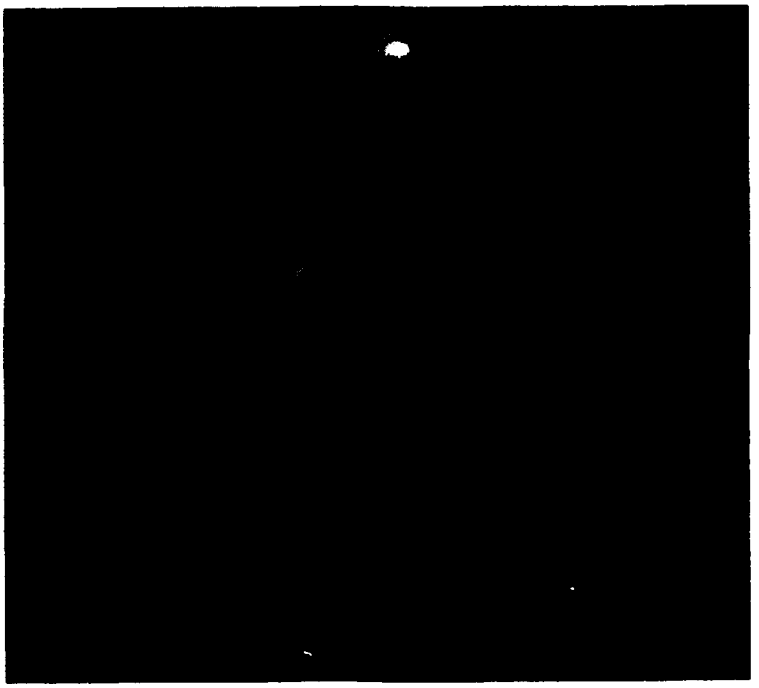

Fig. 5.5 Diamond pellet as seen from above by an unfiltered, open-shutter 35 mm camera, using a reenterent fisheye lens. The diamond enters from the outside midplane of the photo. The extremely narrow track has a blue-white color, unlike either the graphite or hydrogen pellet tracks.

6. REFERENCES

1. M. Lenoci and G. Haas, IPP (Garching), Report III/113 (July 1986).

2. G.G. Spanjers, et.al., "Development of a transient internal probe diagnostic," Rev. Sci. Instrum. 63, 5148 (1992). [Attached as Appendix A]

3. G.G. Spanjers, et.al., "Development of a transient internal probe diagnostic," presented at 9th Topical Conference on High-Temperature Plasma Diagnostics, Santa Fe, N.M., March 15-19, 1992.

4. G.G. Spanjers, J.P. Galambos, M.A. Bohnet, and T.R. Jarboe, "Magnetic field measurements using the transient internal probe," presented at the APS Plasma Physics Conference, Seattle, WA, Nov. 16-20, 1992.

5. M.A. Bohnet, "Development of a two-stage light gas gun," M.S. Thesis, Univ. of Wash., Dept. of Aeronautics and Astronautics, June, 1993.

6. J.P. Galambos, "Remote magnetic field measurements using an optically coupled probe," M.S. Thesis, Univ. of Wash., Dept. of Nuclear Engineering, January, 1993.

7. A.E. Seigel, "Theory of High-Muzzle-Velocity Guns," Interior Ballistics of Guns, H. Krier and M. Summerfield, eds., Progress in Astronautics and Aeronautics, Vol. 66, AIAA, New York, p. 135 (1979).

8. J.J. Rast,"The design of flat-scored, high-pressure diaphrams for use in shock tunnels and gas guns," NAVORD Report 6865, 1961.

9. H.F. Swift and D.E. Strange, "Sabot discard technology," Physics Applications Inc., Internal Report, Oct. 1, 1987.

10. D.W. Roberts, R. Kaita, and F.M. Levinton, Rev. Sci. Instrum. 61 10, 1990.

11. T.W. Petrie, D.N. Hill, J. Baptista, and M. Brown, Rev. Sci. Instrum. 61 11, 1